Jónatas Rodrigues

Development of a structure for a mobile robot

Dissertation to achieve the degree of Master in Mechanical Engineering
in the speciality of Production and Project

September/2017

FACULDADE DE CIÊNCIAS E TECNOLOGIA
UNIVERSIDADE DE COIMBRA

DEPARTAMENTO DE ENGENHARIA MECÂNICA

Development of a structure for a mobile robot

Submitted in Partial Fulfilment of the Requirements for the Degree of Master in Mechanical Engineering in the speciality of Production and Project

Desenvolvimento de uma estrutura para um robô móvel

Author

Jónatas Rodrigues

Advisors

Prof. Doutor Lino José Forte Marques
Prof. Doutor Pedro Mariano Simões Neto

Jury

President	**Professor Doutor Cristóvão Silva** **Professor Auxiliar da Universidade de Coimbra**
Vowel	**Professor Doutor Diogo Mariano Simões Neto** **Professor Auxiliar Convidado da Universidade de Coimbra**
Advisor	**Professor Doutor Lino José Forte Marques** **Professor Auxiliar da Universidade de Coimbra**

Institutional Collaboration

Institute of Systems and Robotic of the University of Coimbra

Coimbra, September, 2017

ACKNOWLEDGEMENTS

One of the most effective ways to gain knowledge is to learn with more experienced people. Throughout this dissertation, several people gave their contribution and I want to express my gratitude:

First, I would like to thank my advisors Professor Doctor Lino Marques and Professor Doctor Pedro Neto for the support, guidance, encouragement and for giving me the opportunity to work in product development. It was one of my objectives when I chose to study mechanical engineering, to become capable of design, project, manufacture and test a new product.

Professor Doctor José Domingos Moreira da Costa for his availability and advice.

I would also like to thank all the people that shared the laboratory with me for the time spent in the collaboration of some tasks and for always giving necessary suggestions to better this dissertation, and specially Sedat Dogru for having patient solving electronic problems with the robot.

A sincere thanks to my friends that always believed in my capacities and kept me focused. To my Parents for their love, understanding and support during my graduate studies. To my Sister for her unconditional friendship.

Abstract

Recently we have witnessed not only the development of mobile robots to perform tasks in dangerous situations for humans but also for activities inside factories or agricultural environments. However, the success of these projects is dependent on the amount of useful research that exists on this subject that results in technology advancements.

The aim of this dissertation is to create a simple modular and reconfigurable mobile robot that can fulfil the need of this equipment in research about that matter. It includes the conceptual and detailed design, simulation, prototyping and testing of a skid-steer robot.

This study starts by defining and classifying outdoor mobile robots according to their structure and locomotion mechanisms. It also refers to the latest prototypes that have been developed in this field, some of them with commercial application.

Furthermore, a study will be done about the forces that will affect the structure, which will be designed with aluminium profiles, and simulated through finite element analysis. This study will not only ensure the development of a viable structure, but also to make it as suitable as possible. This means that the structure must provide the expected characteristics with the lowest possible mass. With that purpose in mind several structures with different types and sizes of profiles will be tested and compared.

The results obtained from the tests performed with the implemented robot are presented in the last chapters, as well as its characteristics. Finally, there is an overlook of all the achievements and conclusions made possible with this research work.

Keywords Skid-steer robots, finite element analysis, field robots, mechanical design.

Resumo

Recentemente, temos assistido não só ao desenvolvimento de robôs móveis para executar tarefas em situações perigosas para humanos, mas também para atividades dentro de fábricas ou ambientes agrícolas. No entanto, o sucesso desses projetos depende da quantidade de investigação que existe sobre esse assunto, resultando em avanços tecnológicos.

O objetivo desta dissertação é tentar criar um robô móvel simples, reconfigurável e modular que possa satisfazer a necessidade desse equipamento na pesquisa sobre esse tópico. Esta dissertação inclui o design conceitual e detalhado, a simulação, a prototipagem e o teste de um robô móvel.

Esta dissertação começa definindo e classificando robôs móveis outdoor de acordo com sua estrutura e mecanismos de locomoção. Também se refere aos protótipos mais recentes que foram desenvolvidos neste campo, alguns deles com aplicação comercial.

Além disso, será feito um estudo dos esforços a que este tipo de robôs serão submetidos para que possa ser iniciado o dimensionamento da estrutura, criada com perfis de alumínio, através de análise de elementos finitos. Este estudo visará não só garantir o desenvolvimento de uma estrutura viável, mas também torná-la tão adequada quanto possível. Isso significa que a estrutura deve proporcionar as características esperadas com a menor massa possível. Com esse objetivo em mente, serão testadas várias estruturas com diferentes tipos de perfil.

Um capítulo sobre os resultados obtidos a partir dos testes feitos ao robô irá concluir com as características do mesmo. Finalmente, há uma visão geral de todas as realizações neste trabalho de pesquisa e possíveis desenvolvimentos futuros.

Key words: robô skid-steer, análise de elementos finitos, robô todo o terreno, design mecânico

Contents

LIST OF FIGURES

LIST OF TABLES

SYMBOLOGY AND ACRONYMS

Symbology

F_u– Force Transmitted by the pulley to the shaft

μ_l – Lateral Friction Coefficient

Fa_l – Lateral Friction Force

m – Mass

g – Gravitational Acceleration

Fa_t – Tangential Fiction Force

M – Momentum created by the motor

H – Horizontal Reaction

V – Vertical Reaction

Ft_{motor} – Tangential force created by the motor

CG – Center of Gravity

a – Horizontal distance between CG and the center of the wheel

b – Vertical distance between CG and the center of the wheel

Acronyms

DEM – Departamento de Engenharia Mecânica

FCTUC – Faculdade de Ciências e Tecnologia da Universidade de Coimbra

ISR – Institute of Systems and Robotics

GPR – Ground Penetrating Radar

NASA – National Aeronautics and Space Administration

DOF – Degree of Freedom

MDOF – Multi Degree of Freedom

FEA – Finite Element Analysis

1. INTRODUCTION

1.1. Background

In 2012 began a project named tiramisu [1] that aimed to provide a set of tools for helping the population facing problems related to mined fields.

The Institute of Systems and Robotics (ISR) of the University of Coimbra was one of the firsts partners of this project, leading the development of Tools for close-in detection focusing its work in the areas of robotics, chemical sensors and sensor fusion for landmine detection.

An autonomous mobile robot with a technology set to detect mines was developed by IRS using a mobile robot named Husky (figure 1.1).

Figure 1.1. Husky with mechanisms that make him prepared to detect mines **[2]**.

The success of this initiative demonstrated the usefulness and versatility of this type of robot. In the same project a skid steer robot was developed with the objective of carrying a GPR-ground penetrating radar for mining detection.

This robot named Hunter (Figure 1.2), never worked properly due to problems it revealed in tests. Deformations in the structure caused misalignment of the belts, so that the vehicle could not move properly.

Figure 1.2. Hunter, inoperative due to problems in mechanisms.

1.2. Motivation

Robotics has achieved its greatest success to date in the world of industrial manufacturing. Robot arms, or manipulators, comprise a 2-billion-dollar industry [3]. Bolted at its shoulder to a specific position in the assembly line, the robot arm can move with great speed and accuracy to perform repetitive tasks such as spot welding and painting. In the electronics industry, manipulators place surface-mounted components with superhuman precision, making the portable telephone and laptop computer possible. Yet, for all of their successes, these commercial robots suffer from a fundamental disadvantage: lack of mobility. A fixed manipulator has a limited range of motion that depends on where it is bolted down. In contrast, a mobile robot would be able to travel throughout the manufacturing plant, flexibly applying its talents wherever it is most effective.

This dissertation focuses on the technology of mobility and more specifically in the development of a novel flexible robot structure.

1.3. Mobile robots applications

Mobile robots can be highly maneuverable and compact being very useful for certainly applications including rescue, investigation, disaster response, agriculture, military, explosive disarmament and exploration of other planets. Nowadays, due to the revolution in the industrial sector, there are innovations regarding the creation of autonomous loading platforms (Figure 1.3), which are intended to assist workers in transporting tools or products inside facilities.

Figure 1.3. Forte, semi-industrial R&D robotic platform **[4]**.

The first robot to explore Martian soil (Figure 1.4) was used in the Pathfinder mission in 1997 and was practically only operated from hearth. It had front and rear cameras and hardware to conduct several scientific experiments. The main objective of this vehicle was to determine the composition of Martian soil.

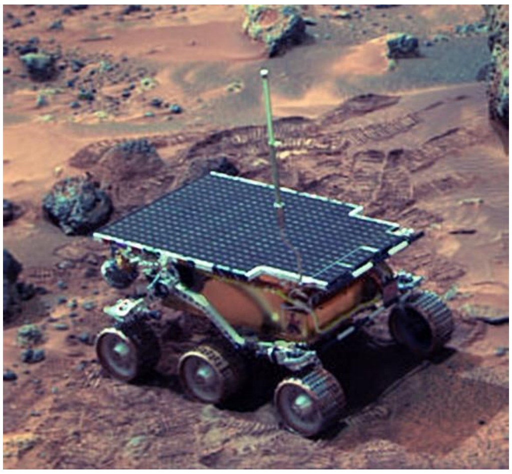

Figure 1.4. Sojourner or Rover **[5]**.

In research, the use of Skid Steer robots is very common due to its simple but robust structure and adaptability. Boston Dynamics developed a robot (Figure 1.5) that aimed not just normal mobility on smooth terrain, but also being able to jump more than nine meters, to overcome obstacles.

Figure 1.5. SandFlea **[6]**.

In health-threatening environments, the use of mobile robots is often the only solution. To respond to the Chernobyl disaster, NASA has built a robot (figure 1.6) capable of obtaining samples in the most affected areas.

Figure 1.6. Pioneer **[7]**.

In agriculture, there are many robots that seek to change the face of agriculture. In figure 1.7 we can see two multi-purpose robotic platforms having four independently steerable drive wheels and the ability to adjust its track width creating highly maneuverability. These can navigate autonomously along plant rows (e.g. dams) in the field, carrying the application module (tool) as it goes.

(a) (b)

Figure 1.7. Mobile robots used in agriculture: a) Bonirob developed by BOSCH Deepfield-Robotics **[8]**, b) Thorvald was desing by SAGA ROBOTICS **[9]**.

In mine Humanitarian Demining, true the lack of other possibilities, robots have been developed, one of them shown in Figure 1.1, but there are several more [10].

1.4. Goals

The aim of this dissertation is the conceptual and detail design, assembly and testing of a skid-steer robot for research purposes. Challenges consist in changing the distance between wheels, therefore it is important that the robot can be reconfigurable. The assembly should also consider different configurations and flexibility to test diverse components such as different wheels or motors.

The fact that there are increasing interest in using mobile robots for vast applications provides motivation for this task.

To summarize, the developed robot should:

-Be simple, modular and reconfigurable

-High stiffness

-Be light in order to save energy

-Be low cost and with easy maintenance

-Usage of standard components

-Fit in doors and inside elevators or be able to climb stairs

This project involves the necessary structural analysis, detailed design, implementation and test of the robot with the following subsystems, which shall be described further on chapter 3 and 4:

- Problems with previous robot
- Mobile robot concept
- Structure development
- Final assembly and manufacturing technologies
- Tests and results

2. STATE OF THE ART

Mobile robots have been built for many proposes with different requirements. Moreover, there are lots of types of structures, forms of locomotion and electronics attached. This state of the art will focus in the mechanical parts of outdoor mobile robots.

A skid steer robot is one of the simplest ways to make a mobile robot, typically consisting of two or four motors, four wheels, a structure, and a set of other components that allow the connections and power transmission. This type of robot is composed of fixed axes, the rotation of the robot is achieved by steer when two wheels on one side of the vehicle move in one direction and the other in the opposite direction.

2.1. Structure

Recently the interest for mobile robots has been emerging, consequently many gadgets have been developed to improve his utility, making the technology relatively complex. Therefore, the robot´s structure is sometimes overlooked because is not typically the aim of the project. Nevertheless, to facilitate experiences and to achieve good results a well-made robot can be very helpful.

The most used materials in mobile robots are aluminium and steel. These materials provide resistance, and durability. Some mobile robots are built with welded structure, others only using screws in connections, and to fix the components it is usually used screws.

The following parts will give examples and explain the three types of structures that were found in market and in research projects of outdoor robots.

2.1.1. Flexible structure

Flexible structure means that there are one or more degrees of freedom. Usually this kind of mobile robots aims to gain traction and adaptability to the ground. In figure 2.1 these robots can rotate the part of the structure that connects both wheels of one side of the robot independently from the rest of the robot.

The main problem with robots made with this kind of structure is the payload. These robots in figure 2.1 can only carry 5 kg and generally, these robots have very low load capacities.

(a)

(b)

Figure 2.1. Skid Steer robots with flexible structure: a) Nomad 4WD Off-Road Chassis Kit **[11]**, b) Gears EdS-Heavy Metal Articulating Chassis (left) and Gears EdS - Surface Mobility Platform (right) **[12]**.

2.1.1. Rigid structure

Mobile robots with rigid structures are the type of robots that have a better relationship between load capacity and their own weight. Some robots with simple structures as Hangfa Navigator C2 in figure 2.2, can carry 100 kg with a weight of 40 kg. Super mega bot in figure 2.2 can move up to 6.7 m/s, carry 113 kg with a weight of 100 kg and his ground clearance is 140mm. It has also a towing capacity of 1350 kg.

(a) (b)

Figure 2.2. Sid steer robots with rigid structure: a) Hangfa Navigator C2 Robot Platform **[13]**, b) Inspectorbots Super Mega Bot **[14]**.

Warthog in figure 2.3 is a big robot platform, designed for agricultural activities or heavy duties, having a payload of 272 kg and ground clearance of 254 mm but with a weight of 280 kg and with 1.38 m of width, consequently, is not set for indoor usage.

Figure 2.3. WARTHOG, amphibious unmanned ground vehicle from Clearpath **[15]**.

2.1.2. Modular and Reconfigurable

Modularity is defined as the characteristic of being constructed of a set of standardized components which usually can be interchanged. Reconfigurability is the ability to rearrange a robot's physical components. It can be done dynamically meaning that the robot may reconfigure itself “on-the-fly." Its opposite is manually reconfigurable which means another agent (human or robot) must reconfigure the robot.

There has been some study in modular and reconfigurable mobile outdoor robots, especially with the purpose of being able to carry or attach different components in the robot. The Small Robotic Farm Vehicle (figure 2.4) is a lightweight and energy efficient robotic vehicle with a configurable and modular design, enabling interchangeable implemented units to span between the modular side units. This modular design allows the Small Robotic Farm Vehicle to undertake a range of agricultural tasks and experiments, including seeding.

Figure 2.4. Small Robotic Farm Vehicle **[16]**.

The reconfigurability of the position of the wheels has been made with research objective. An example is Robot Component Kit (RCK) which allows the assembling of a wide range of different robot driving platforms by simple combination of base components from a component kit box (figure 2.5). The purpose of the RCK is the provision of a ready to use robot driving platform for robot research and for education in robotics at university laboratories.

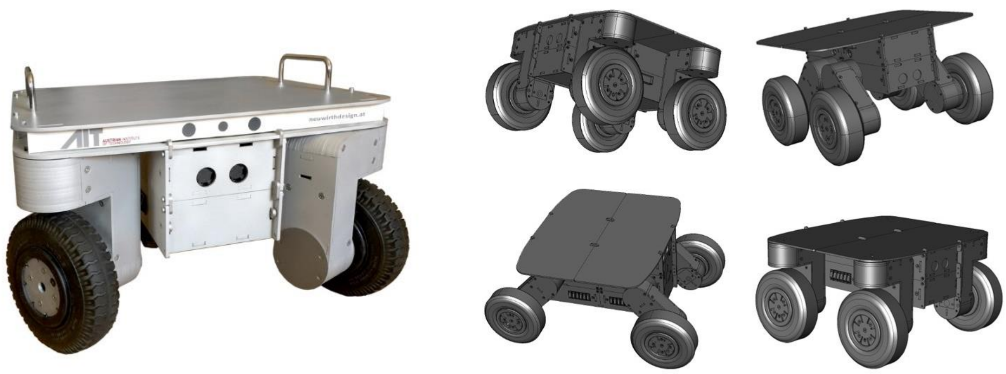

Figure 2.5. Robot Component Kit **[17]**.

In figure 2.6 is presented an example of a robot that can reconfigure itself. Autonomous omnidirectional mobile vehicle was engineered with a full focus on stiffness, reusability, and multi-degree-of-freedom (MDOF), which prove them better over conventional (i.e., 2-DOF) vehicle. For example, MDOF vehicle can travel sideway, skew, and is able to take on the spot 360˚ turn as well negotiate tight turn more easily, which provide ease to move safely in meaningful and purposive manner in between row and column of crops. Each wheel is propelled and steered by an individual motor, which provide ease to control it.

Figure 2.6. Modular Multipurpose Omnidirectional Autonomous Mobile Robotic Platform **[18]**.

Makeblock is an aluminium extrusion based construct platform that can be used to build robots (figure 2.7). These robots are easily mounted and reconfigurable. Has they have low load capacity and fragile structures, these are mainly used by students and children.

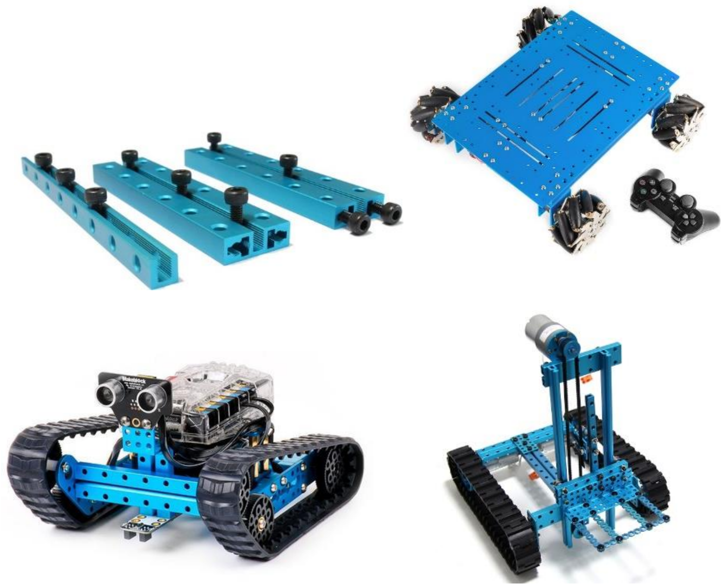

Figure 2.7. Robots made with parts from Makeblock **[19]**.

2.2. Locomotion Mechanism

Mobile robots locomotion is usually driven by wheeled mechanisms or by articulated legs. In general, legged locomotion requires higher degrees of freedom and therefore greater mechanical complexity than wheeled locomotion. Wheels, in addition to being simple, are extremely well suited to flat ground. As figure 2.8 shows, on flat surfaces wheeled locomotion is one to two orders of magnitude more efficient than legged locomotion. The railway is ideally engineered for wheeled locomotion because rolling friction is minimized on a hard and flat steel surface. But as the surface becomes soft, wheeled locomotion accumulates inefficiencies due to rolling friction whereas legged locomotion suffers much less because it consists only of point contacts with the ground. This is demonstrated in figure 2.8 by the dramatic loss of efficiency in the case of a tire on soft ground.

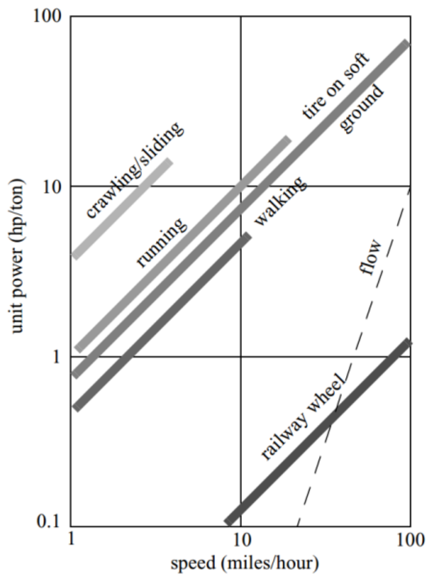

Figure 2.8. Specific power versus attainable speed of various locomotion mechanisms **[3]**.

There is no ‘ideal’ drive configuration that simultaneously maximizes stability, manoeuvrability, and controllability. Each mobile robot application places unique constraints on the robot design problem. Furthermore, will be shown robots having different locomotion mechanisms.

2.2.1. Wheels

The wheel has been by far the most popular locomotion mechanism in mobile robotics and in man-made vehicles in general. It can achieve very good efficiencies, as demonstrated in figure 2.8, and does so with a relatively simple mechanical implementation. In addition, balance is not usually a research problem in wheeled robot designs, because wheeled robots are almost always designed so that all wheels are always with ground contact. When more than three wheels are used, a suspension system is required to allow all wheels to maintain ground contact when the robot encounters uneven terrain.

The major types of wheels are standard wheel shown in figure 2.9 used by Dr. Robot Jaguar, and steered standard wheel used by Seekur. The standard wheel has a roll axis parallel to the plane of the floor and can change orientation by rotating about an axis normal to the ground through the contact point. A fixed standard wheel is mounted directly to the robot body. When the wheel is mounted on a rotational link with the axis of rotation passing through the contact point, we speak of a steered standard wheel. A variation which reduces rotational slip during steering is called the lateral offset wheel. The wheel axis still intersects the roll axis but not at the contact point. The caster offset standard wheel, also known as the castor wheel, has a rotational link with a vertical steer axis skew to the roll axis. The key difference between the fixed wheel and the castor wheel is that the fixed wheel can accomplish a steering motion with no side effects, as the centre of rotation passes through the contact patch with the ground, whereas the castor wheel rotates around an offset axis, causing a force to be imparted to the robot chassis during steering [20].

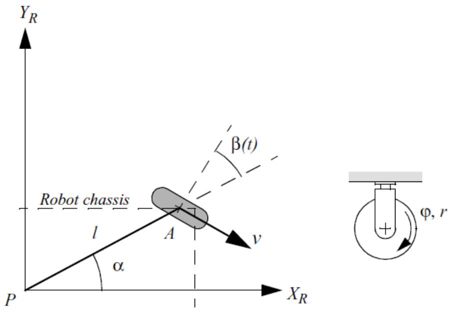

(a)

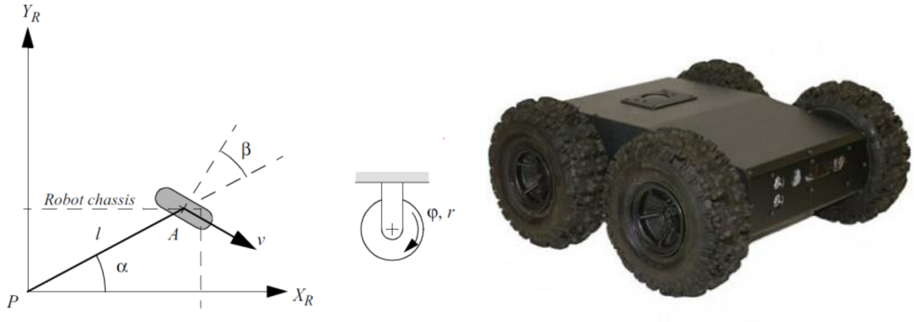

(b)

Figure 2.9. Kinematics constrains **[3]** and examples of mobile robots using four wheels as locomotion mechanism: a) steered standard wheel, Adept Mobile Robots Seekur system **[21]**, b) fixed standard wheel, Dr. Robot Jaguar 4x4 Mobile Platform **[22]**.

Figure 2.9 depicts a fixed standard wheel and indicates its position pose relative to the robot's local reference frame $\{X_R, Y_R\}$. The position of is expressed in polar coordinates by distance l and angle α. The angle of the wheel plane relative to the chassis is denoted by β, which is fixed since the fixed standard wheel is not steerable. The wheel, which has radius r, can spin over time, and so its rotational position around its horizontal axle is a function of time t: $\phi(t)$

The steered standard wheel differs from the fixed standard wheel only in that there is an additional degree of freedom. The orientation of the wheel to the robot chassis is no longer a single fixed value, β but instead varies as a function of time: $\beta(t)$

Robots can have more wheels, as we can see some examples in figure 2.10, increasing stability and ground contact. These have a more complex structure and because of the larger contact between wheels and ground, it results in more friction, and waste of energy.

(a) **(b)** **(c)**

Figure 2.10. Mobile robots with six wheels: a) 6WD Wild Mobile Platform **[23]**, b) Super Droid Robots 6WD All Terrain Robot Platform **[24]**, c) Custom RC 6WD Robot with Snow Plow **[25]**.

The robot on the left is provided with 6 powerful steel geared motors, spiked tractor tyres and a "Super Twist" suspension system to keep all wheels on the ground. Despite having very good traction, it is not prepared for heavy payloads. Those other robots are straight rigid structures prepared for heavy duties. We can see RC 6WD with a snow plow prepared to remove any snow or trash from the road.

2.2.1. Tracked robot

Robots that make use of tread have much larger ground contact patches, and this can significantly improve their maneuverability in loose terrain compared to conventional wheeled designs. However, due to this large ground contact patch, changing the orientation of the robot usually requires a skidding turn, wherein a large portion of the track must slide against the terrain. The disadvantage of such configurations is coupled to the slip/skid steering. Because of the large amount of skidding during a turn, the exact centre of rotation of the robot is hard to predict and the exact change in position and orientation is also subject to variations depending on the ground friction. This is the trade-off that is made in return for extremely good maneuverability and traction over rough and loose terrain. Furthermore, a slip/skid approach on a high-friction surface can quickly overcome the torque capabilities of the motors being used. In terms of power efficiency, this approach is reasonably efficient on loose terrain but extremely inefficient otherwise.

This type of locomotion can also be used with double-track, and not adding more motors, as explained by Cheong Hee Lee [26]. This uses a passive rotational mechanism that improves the energy efficiency because it does not need an additional motor to change the track configuration. This passive concept (figure 2.11) also improves environmental adaptability.

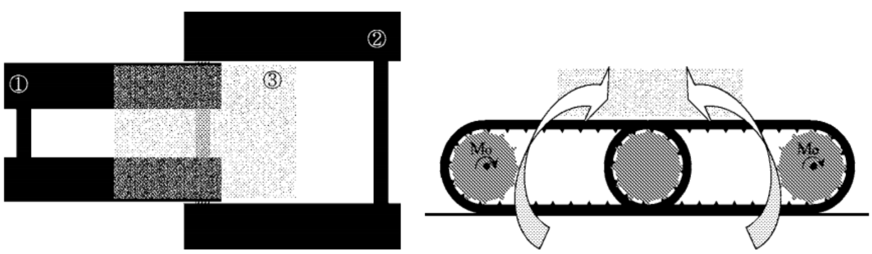

(a) (b)

Figure 2.11. Structure of the double side mechanism: a) top view and b) side view.

Both these vehicles in figure 2.12 can without difficulty climb stairs. Dr. Robot Jaguar is capable of climbing up to 300 mm with ease due to is arms and Super-Size HD Tracked Tank can carry 100 kg. XBOT can carry 350 kg, but ita weight is 500 kg.

(a) **(b)** **(c)**

Figure 2.12. Tracked mobile robots: a) Super-Size HD Tracked Tank Robot **[27]**, b) Jaguar V4 Tracked Mobile Robotic Platform **[28]**, c) XBOT All Terrain Tracked Mobile Robot **[29]**.

A similar type of triangular-tracked mechanism like XBOT uses, can be applicated in normal skid-steer robots by utilizing a concept described by Angelo Afanador [30]. A motor vehicle accessory affixable to a standard predetermined vehicle wheel hub comprising a frame assembly and a track assembly (figure 2.13).

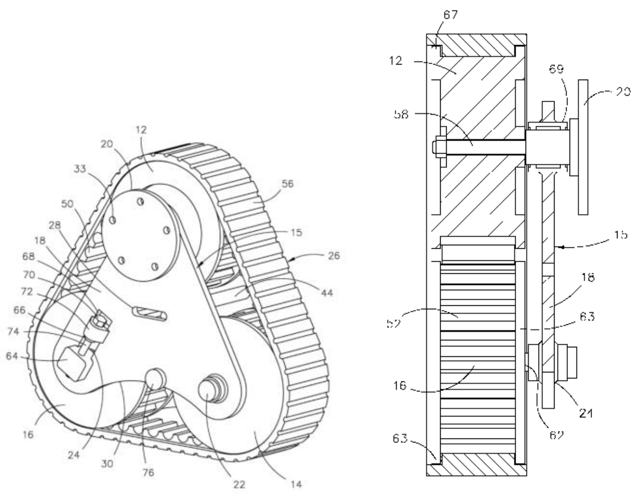

Figure 2.13. Triangle-tracked wheel

2.2.2. Omni-directional wheel

The omni-directional wheel was first patented in 1919 by J. Grabowiecki. US patent 1305535, "Vehicle wheel", issued 1919-06-03. But without practical application.

More recently Steven D. Potter, US 7980335 in 2009, developed a omni-directional wheel which includes a hub rotatable about a wheel axis and a first row of angled rollers about the hub each rotatably supported by the hub. There is at least a second row of angled rollers about the hub each also rotatably supported by the hub. The rollers of the second row are axially offset along the wheel axis from the first row, and rotationally offset from the first row about the wheel axis, and not coaxial with the rollers of the first row. This patent has been used by Vehicle Technologies Inc. to produce some useful robots shown in figure 2.14.

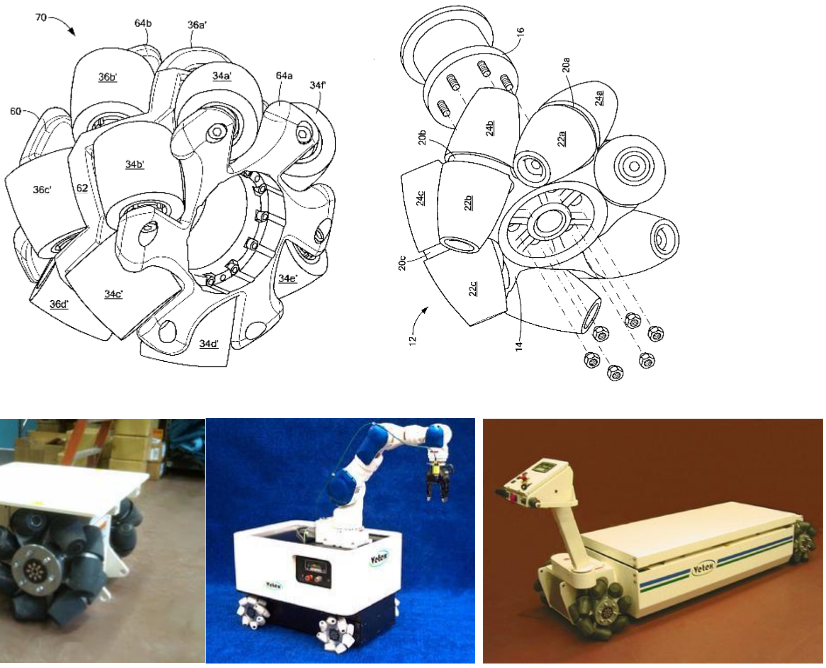

Figure 2.14. On the top, we can see two examples of this type of wheels **[31]** and on the bottom, we have three different robots developed by Vehicle Technologies Inc. **[32]**.

Omnidirectional movement is of great interest for complete manoeuvrability. For example, when a robot has four wheels, if they spin “forward” or “backward” the robot as a whole moves in a straight line forward or backward, respectively. However, when one diagonal pair of wheels is spun in the same direction and the other diagonal pair is spun in the opposite direction, the robot moves laterally. It can also spin around its vertical axis if the wheels on the left spin in one direction and those on the right spin in the opposite direction.

Kuka Roboter Gmbh is other company that in recent years has been focusing in this technology, also having a patent regarding a mobile robot with omnidirectional wheels and one arm on the top [33]. This type of robot (figure 2.15) combines strength with flexibility, being capable of handling many kinds of objects, inside a factory, alongside humans.

Figure 2.15. KUKA youBot **[34]** on the left, mainly used in research and teaching. It consists of an omnidirectional mobile platform on which a five-axis robot arm with a two-finger gripper is installed. On the right KUKA KMR iiwa **[35]**, having the same technology but more prepared for practical applications.

A basic omni-directional wheel also named mecanum wheel consists of a series of rollers attached to its circumference (figure 2.16). These rollers typically each have an axis of rotation at 45° to the plane of the wheel and at 45° to a line through the centre of the roller parallel to the axis of rotation of the wheel. Nowadays this concept is not under any patent.

Figure 2.16. Hangfa Navigator Q2 Robot Platform, with four 45 degrees QMA-15 omni wheels **[36]**.

2.1. Overview and performance comparison

Mobile robots shown before represent most of the characteristics and specifications available in market and some solutions only implemented in research projects. Those platforms are useful for several situations, and use different features to be reliable on different applications.

The Table 2.1 sums up the characteristics of some of the robots referenced in this state of the art, representing the main technologies used in field robots.

Table 2.1. Comparison of different outdoor mobile robots.

	Husky	Super Mega Bot	Small Robotic Farm Vehicle	6WD All Terrain	Jaguar V4 Tracked	Seekur	Hangfa Navigator Q2 Robot Platform
Weight (kg)	50	113	400	68	< 30	300	32
Payload (kg)	75	100	200	68	15	-	80
Max. Speed (m/s)	1	6.7	2.8	1.3	1.5	1.8	1.2
Width (mm)	670	838	3000	990	700	1300	481
Ground Clearance (mm)	130	140	320	120	150	180	73
Climb Stairs	No	No	No	No	Yes	No	No
Modular	No	No	Yes	No	No	No	No
Omni-directional	No	No	No	No	No	Yes	Yes

Many of the robots in table 2.1 have more than the payload that we need. To fit inside the elevator the width should be less than 850 mm, which is also achieved by most of them. The problem with mobile robots available in market is that none of them offers reconfigurability and very few are modular. As it was explained before there are some research projects where reconfigurable robots were developed, but like Small Robotic Farm Vehicle, those were made with a specific purpose, and their reconfigurability does not extend to the all structure, it only applies to some parts of the robot.

3. MOBILE ROBOT DEVELOPMENT

The following flowchart (figure 3.1) shows the aspects taken into account and the steps that were followed in the development of this robot.

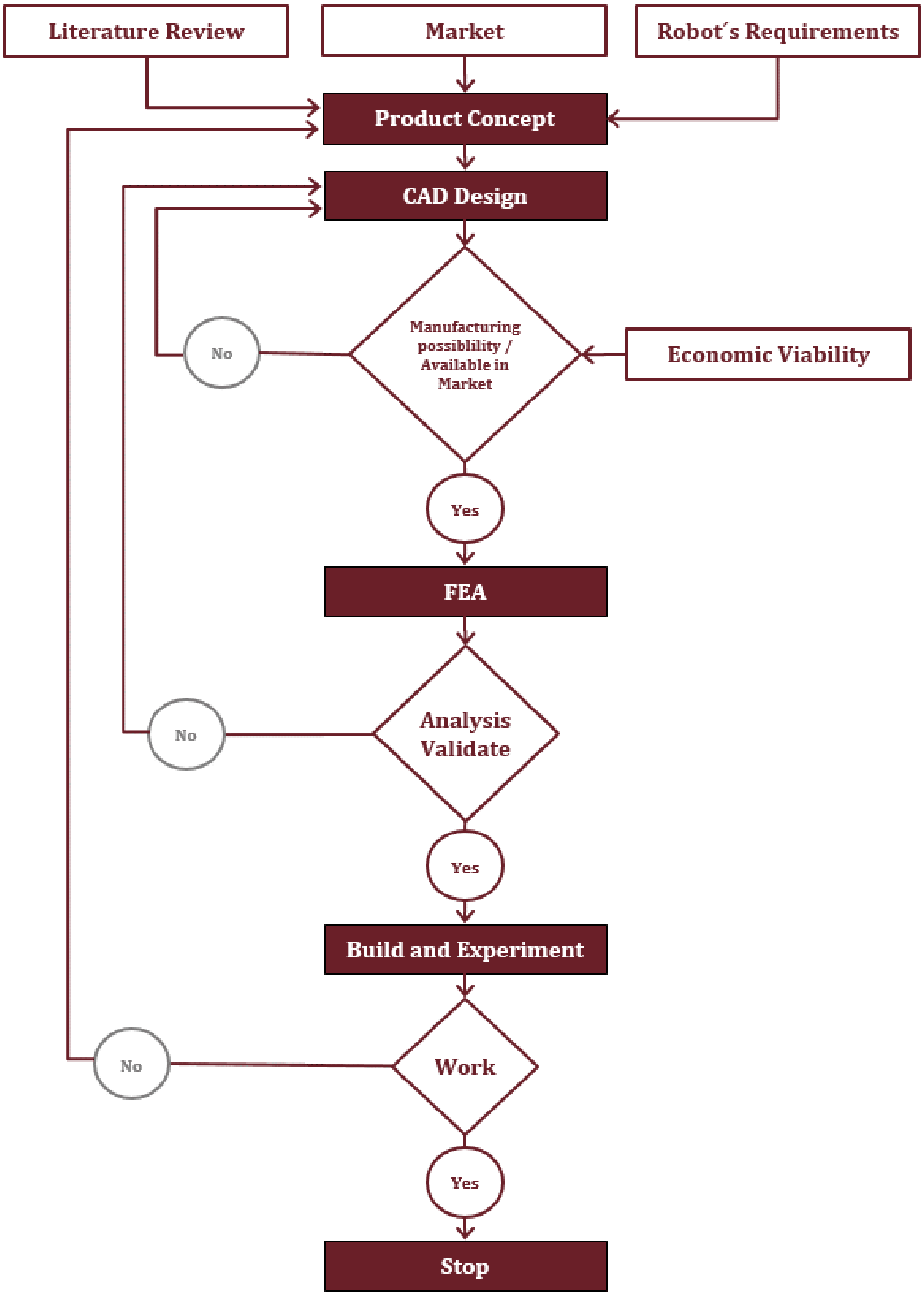

Figure 3.1. Flowchart of Mobile Robotic Platform Design and Development.

3.1. Problems with the previous robot

First, we need to understand the problems in the previous robot (figure 1.2). This robot was made with an aluminium coffin-shaped structure, and the general thickness was two millimetres. Despite this does not seem enough to make an appropriate structure, we only know if it will work or not if the worst challenging conditions are considered in our project.

One simulation was made using SolidWorks (figure 3.2) in which the structure had applied a remote load that described the weight of an object that this robot was supposed to carry at the time that the design was made.

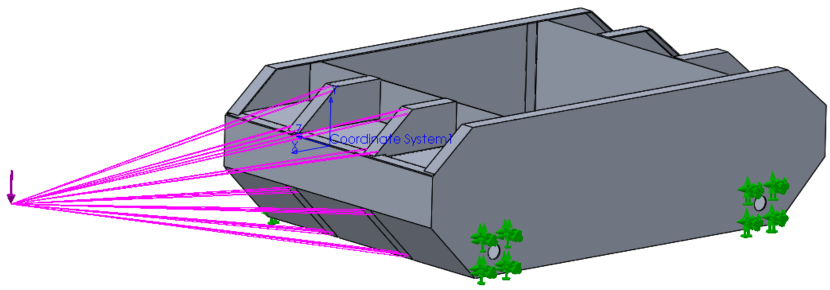

Figure 3.2. Simulation made to secure the safety of the structure with a remote load.

The structure will be submitted to forces originated in pulleys by the movement of the belt, the friction caused by skid steer movement and the total payload.

A skid steer robot needs at least two motors, because both sides of the robot need different speeds to create rotation. Consequently, this project was planned with the usage of two motors and having two belts, one between the shafts of each side of the robot in order to create traction in all four wheels. But the transmission of movement between the motor and the shaft was obtained using pulleys and another belt (figure 3.3), creating forces that were transmitted to the structure. This force transmitted by the pulley to the shaft (F_u) can be obtained by the following equation:

$$F_u = \frac{Torque}{Radius\ of\ the\ pulley} \tag{3.1}$$

From equation 3.1 it can be seen that the force created by the pulley is inversely proportional to the radius of the pulley. Furthermore, it was used on the former project a pulley with only 45 mm of radius. This pulley will be replaced with a bigger one.

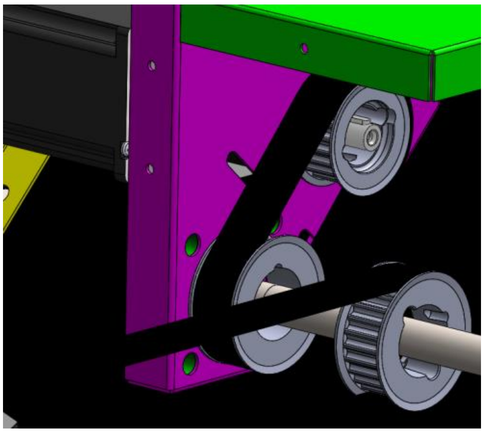

Figure 3.3. Motion transmission between the motor and the wheel using two pulleys and one belt.

3.2. Mobile robot concept

Bearing in mind the lack of stiffness of the preceding structure, was thought about creating a new chassis using aluminium bars, connecting all the main parts of the robot, and absorbing all loads. With the purpose of reducing the forces applied in the structure by the belts, the connection between the motor and the shaft will use a coupling as it is shown in figure 3.4. Those solutions make the robot stronger and less exposed to deformations.

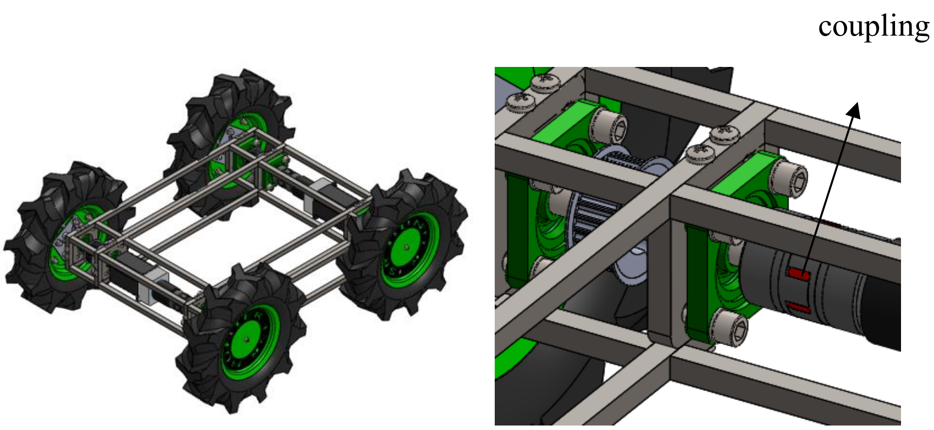

Figure 3.4. On the left the first concept for the new mobile robot and on the right the use of a coupling to connect both shafts of the wheel and motor.

3.3. Structure development

One of the ideas for this robot was the possibility of reconfigurability. The structure should also be light and strong. Aluminium is cheap, light and resistant, being one of the most widespread materials for many applications. We found in aluminium profiles the best solution for our structural necessities. This product doesn't need welding to assemble. It can all be mounted using mainly screws and nuts with standard specific connections, available in the market.

There are lots of profile sizes and lots of connections on the market, so if we understand the requirements, which we will attend next, it will be easy to find the right solutions. The characteristics of the material used are introduced in table 3.1.

Table 3.1. Extruded profile Al Mg Si 0.5 F 25.

Tensile strength	$245\ MPa$
Yield Point	$195\ MPa$
Density	$2.7\ kg/dm^3$
Modulus of elasticity E	$70000\ MPa$
Modulus of rigidity G	$25000\ MPa$
Hardness	$75\ HB$

3.3.1. Analysis of the loads

We need to make sure that the robot works in all situations, therefor, the worst-case scenario will be when the robot is starting to rotate around itself with the maximum payload. If the robot can resist these kinds of efforts, it can be operational in every other situation.

Loads are transmitted to the structure through the bearings that are holding the shafts. Reactions in bearings will be calculated to obtain the tensions and deformations in the structure using static simulation in SolidWorks.

The robot rotation is created by skid steer when both wheels of one side of the robot rotate in one direction and the other wheels rotate in the opposite direction. This movement create friction between the ground and the wheels, not only in the rolling direction but also in the lateral side of the wheels.

Dogru and Marques in [37], presented a way to characterize power consumption of skid steer wheeled robots through estimation of the friction coefficient. They ran tests on various indoor and outdoor surfaces. They conclude that a skid steered vehicle's energy efficiency decreases with the decreasing of the radius of curvature. This decrease also happens with decreasing speeds during skid motion.

On this paper, their bigger estimation of lateral friction coefficient (μ_l) was 0.49 on concrete. This result was obtained with a velocity of 0.2 m/s, being a dynamic friction coefficient. The static friction coefficient should be bigger, but it was not found any results for this type of coefficient or any others in worst conditions. Therefore, for this project, we estimate that the coefficient that the robot is going to be exposed to, will not be more than 1 and it will be used for our project calculations, to calculate lateral friction force (Fa_l) according with equation 3.2.

$$Fa_l = m\mu_l g cos\alpha \tag{3.2}$$

One of the most important loads is the one created by the belt. Using equation 3.1, it is obtained the force created by a new selected pulley with 0.9 mm of diameter.

$$F_u = \frac{168}{0.045} = 3733.33\ N$$

Figure 3.5 show the forces ($Fa_{lateral}, Fa_{tangential}, F_u$) and momentum ($M$) applied on the shafts in the situation described before and reactions in horizontal (H_1, H_2) and vertical (V_1, V_2) planes of the robot. To resolve the equations bellow we only need to know the characteristics of the motors that we are going to use, and the maximum mass combined of the robot and the payload.

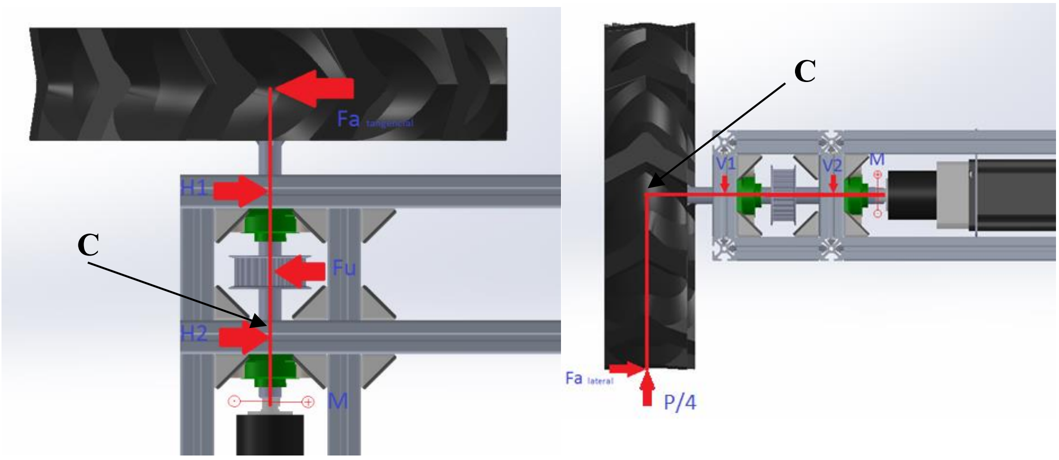

Figure 3.5. On the left: top view (horizontal) of one quarter of the robot, and front view (vertical) on the right, both with forces and momentums applied.

The motors where already bought, and we will only check if they can move the robot in the worst-case scenario. To assure that, the moment created by the motors, must overcome the friction created by the ground.

In figure 3.6 the situation is exposed with a radius of curvature equal to zero. It shows the forces created by the motor in each wheel Ft_{motor}, in blue, and the friction forces Fa_l that counter the previous ones, in red.

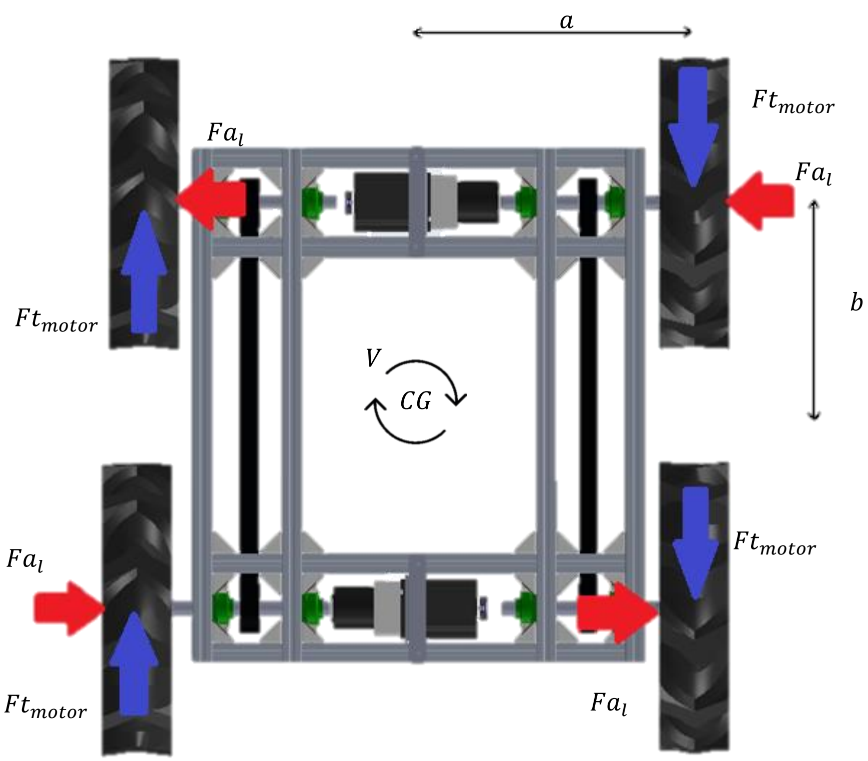

Figure 3.6. Top view of the robot; movement around his geometric centre with forces in each wheel.

The shaft and the wheel have 20 mm and 420 mm of diameter, respectively. The motors peak torque is 4.2 Nm and the reduction of the gear box is 40 times. Therefore, the tangential force created in each wheel is:

$$Ft_{motor} = \frac{Torque}{Radius\ of\ the\ wheel} = \frac{\frac{4.2}{2}\times 40}{\frac{0.420}{2}} = 400\ N \tag{3.3}$$

To calculate how much friction force can the motors overcome, in the limit, the sum of the momentums around the centre of geometry (CG) should be zero.

$$\begin{gathered} \sum M = 0 \ \Leftrightarrow \\ \Leftrightarrow 4\times Ft_{motor}\times a = 4\times Fa_l\times b \\ \Leftrightarrow Fa_l = 452N \\ \Leftrightarrow Fa_{l_{Total}} = 1806N \end{gathered} \tag{3.4}$$

Using equation 3.2 result, it will be obtained the mass that can generate the force calculated above.

$$m = \frac{Fa_{l_{Total}}}{\mu_l g cos\alpha} \Leftrightarrow$$

$$\Leftrightarrow m = \frac{1806}{1\times 9.81} = 184\ Kg$$

We want a robot with a payload of 100 kg. Consequently, we can construct a robot with 84 kg tops. The robot´s structure should be as stronger as we can make, consequently, it was made a first concept of this robot (figure 3.7) to have an idea of the mass that we have of our disposal to the aluminium main structure.

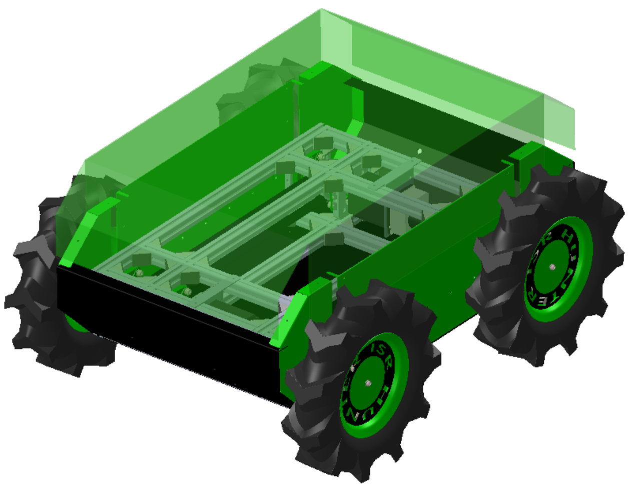

Figure 3.7. First concept of the robot, with all the information at the time. [28/4/2017]

Table 3.2. Parts and masses of the first design

Part	Mass [kg]
Profiles	15
Connections	15
Pulleys; couplings; Bearings	7
Structure coverage	6
Motors; Batteries; Controllers; Computer;	9
Wheels and shafts	24
Total	76

With the following masses based on this first concept, we can conclude that the profile bars shall have around 15 kg.

Now we can present static equations according with figure 3.5 in which the friction force direction is different for each pair of wheels.

$$\begin{cases} \sum My = 0 \\ \sum Fy = 0 \end{cases} \tag{3.5}$$

Using equation 3.3 for horizontal reactions:

$$\Leftrightarrow \begin{cases} H_2 \times 0.1 \mp F_u \times 0.05 + F_t \times 0.1 = 0 \\ H_1 + H_2 \mp F_u + F_t = 0 \end{cases}$$

$$\Leftrightarrow \begin{cases} H_2 = 1466\ N \\ H_1 = 2667\ N \end{cases} \vee \begin{cases} H_2 = -2260\ N \\ H_1 = -1073\ N \end{cases}$$

Using equation 3.3 for vertical reactions:

$$\Leftrightarrow \begin{cases} V_1 \times 0{,}11 + V_2 \times 0{,}21 \mp F_a \times 0{,}21 = 0 \\ V_1 + V_2 - \dfrac{P}{4} = 0 \end{cases}$$

$$\Leftrightarrow \begin{cases} V_2 = -1220\ N \\ V_1 = 1465\ N \end{cases} \vee \begin{cases} V_2 = 680\ N \\ V_1 = 435\ N \end{cases}$$

Knowing all reactions that will affect the robot´s structure, we are now prepared to dimension the size of the profile and the configuration of the structure.

3.3.2. Simulation characteristics

The problem with the simulation made for the previous robot was that it was only describing half of the problem. In this section, we will explain some of the simulations made to describe the worst-case scenario and the characteristics of those simulations.

It will be used a SolidWorks static simulation to describe the scenario when the robot will start the rotation around itself, right before it starts moving.

The usage of simulations to help in dimensioning requires that the simulation consumes not very much time, because it may be necessary to do a lot of simulations for different structures and with different considerations. The first simulation made only had the structural part that it is being dimensioned (figure 3.8), so we could have a simple simulation.

In these types of simulations, we need to introduce restrictions to the movement. Therefore, it was obvious that the bearings are the parts that don’t let the structure move, because they are connected to the wheels that are in contact with the floor. It was necessary to introduce the external forces created by the motors and the payload. The restrictions were in the wholes that will be in contact with the screws, a force was applied on top of the structure and a torque was applied on all external faces of the profiles.

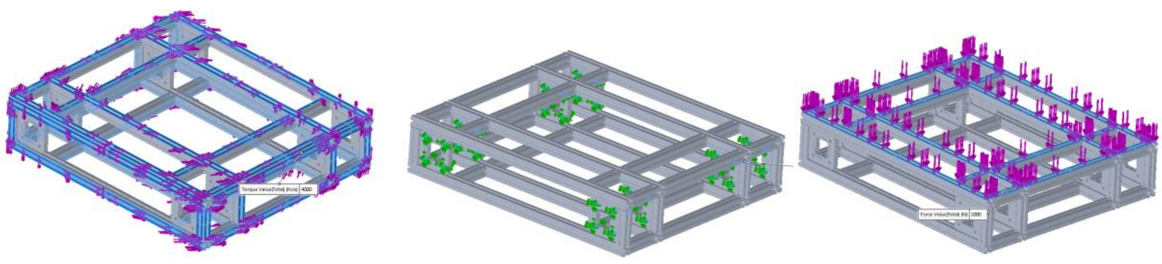

(a) **(b)** **(c)**

Figure 3.8. Simulation made only with the structure that is being developed: a) momentum in purple, b) restrictions in green, c) force representing payload in purple

The deformation of the structure (figure 3.9) would be almost zero near the restrictions and as the torque was applied in most of the structure. It was optimistic compared with the real situation.

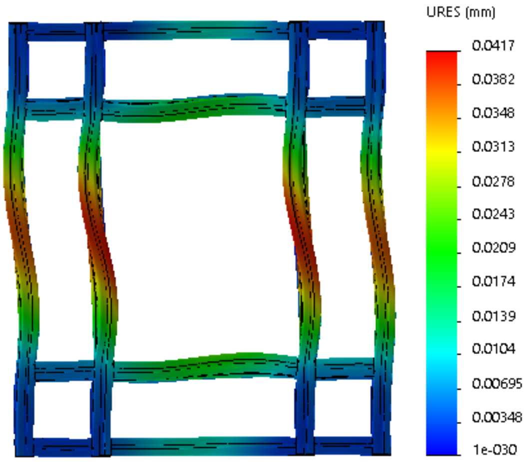

Figure 3.9. Deformation result of the study shown in figure 3.8, top view.

The solution found to make a better description of what it is happening with the structure, was to apply the calculated forces in bearings and then make auxiliary parts to replicate the bearings shafts and wheels, and create restrictions between the wheels and the ground (figure 3.10). The size of the shafts bearings and wheels was very similar or even equal to the real one. The material used for these parts was ANSI 1045 Steel and the wheel was made as a shell with 5 mm thickness.

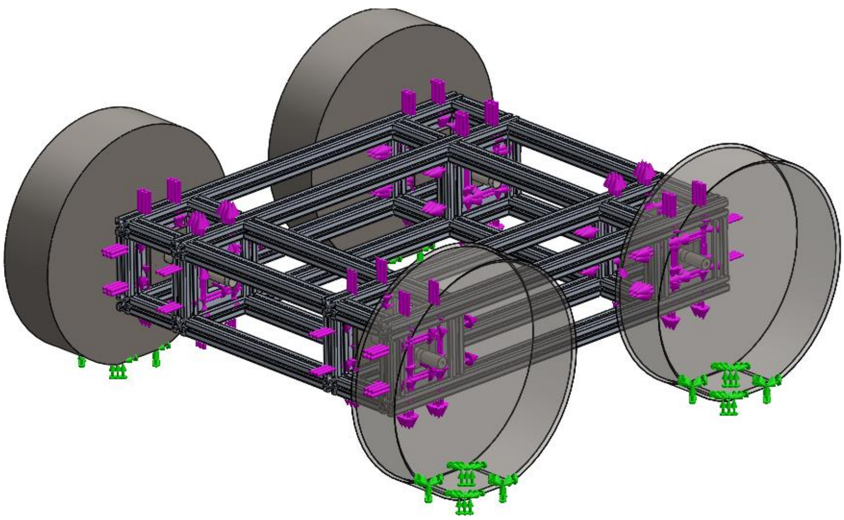

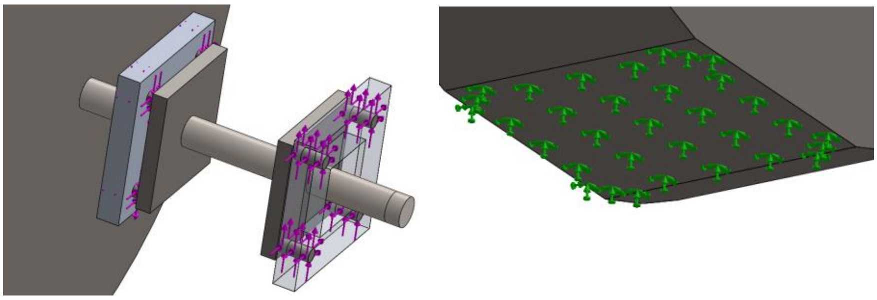

Figure 3.10. Model of the robot, forces in purple and restrictions in green.

This simulation will be made with a safety factor of two which means that all forces applied will be the double of what was calculated with equation 3.3. These restrictions are all fixed geometry, in all directions.

The simulation leads to the deformation shown in figure 3.11, which should be like what will happen with the structure.

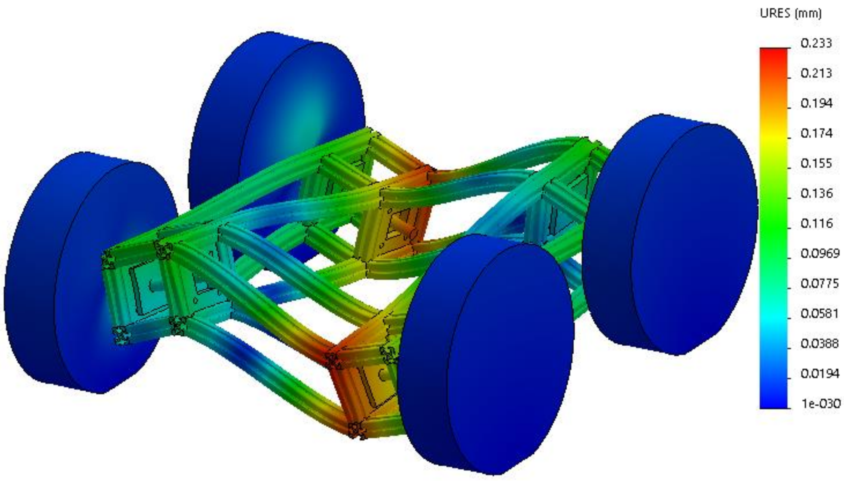

Figure 3.11. Deformation result for the model developed (figure 3.10).

In SolidWorks static simulation there are two mesh types which are standard mesh and curvature based mesh. Curvature based mesh is usually more appropriate for parts with edges and curve surfaces.

Before choosing the mesh type it was done some simulations to test the right mesh type for the next studies. The structure utilized was like the one used in figure 3.7 using 40 mm profiles.

To compare the two mesh types, we need to evaluate mesh quality. It can be done by analysing the aspect ratio of the elements. The best aspect ratio is 1, and it gets worse whenever we move farther away.

Three studies were made, first with standard mesh, using default element size for the most complex part of the assembly. The second study was done with the purpose of having similar number of elements, and the third aimed to have the same meshing time. Results will be shown in table 3.3:

Table 3.3. Different types of meshing and parameters for the same structure.

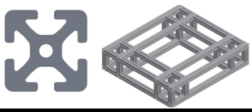	**Standard Mesh**	**Curvature-Based Mesh**	
Jacobian Points	4	4	4
Maximum Element Size [mm]	-	21.5	12.5
Minimum Element Size [mm]	-	4.3	2.5
Element Size [mm]	4.53	-	-
Tolerance [mm]	0.23	-	-
Total Nodes	4418281	4342530	8348196
Total Elements	2644272	2655730	5226249
Time [hh:mm:ss]	00:08:15	00:04:05	00:07:56
Maximum Aspect Ratio	49.28	86.65	33.22
Percentage of Elements with Aspect Ratio < 3	91.7	71.5	87.5
Percentage of Elements with Aspect Ratio > 10	0.101	1.35	0.107
Total Solution Time	00:06:36	00:13:35	00:31:52
Maximum Displacement [mm]	0.16	0.15	0.16
Maximum Von Mises Tension [MPa]	36.5	28	32.2

Creating a mesh with approximately the same number of elements takes approximately twice as much as a standard mesh, although this time is retrieved by the simulation time. On the other hand, using roughly the same time to create a mesh, we are able to have approximately double the elements in a curvature based mesh comparative to the standard mesh, but as we can see the time required for the simulation will be more than five times greater.

In terms of the aspect ratio of the elements, we see that with the same number of elements, we obtain not only a lower maximum aspect ratio for the standard mesh but also a higher percentage of elements with an aspect ratio value of less than 3 and a smaller percentage of elements greater than 10, making the mesh of the standard type with better quality. Comparing both the standard and curvature based meshes that took approximately the same time to be created, the maximum aspect ratio is higher for the standard mesh, but there is a greater percentage of elements with an aspect ratio of less than 3 for the standard mesh and also a smaller percentage for aspect ratio greater than 10.

Looking at the results, we can see that the most refined mesh of the curvature-based mesh has values closer to the results of the standard type mesh.

The standard type mesh achieves the best time combined between time to create the mesh and time to obtain results, it also has more percentage of elements with aspect ratio of less than 3 and less percentage of elements with aspect ratio greater than 10, also, the results are closer to the more refined curvature-based mesh.

To conclude, the mesh type used will be solid mesh, using standard mesh. The element size utilized will be the one suggested by SolidWorks for the most complex part, which basically means to create a study for the most complex part of the assembly and copy the properties suggested. Being a solid study, the elements used by SolidWorks are tetrahedral, with high quality.

Results and structure chosen will be explained in the next part.

3.3.3. Simulation results

Having developed a model to evaluate the structure performance, it is now time to focus on the different profile sizes and possible configurations for the structure.

In annex A will be explained the first approach made to see how different structures will behave with the same profile.

We will see that in terms of tensions, almost every profile is in the safe side, however it is important that the deformation is as low as we can get, to have reliable mechanisms, because that was the reason that made the last robot inoperable.

It was assembled specific configurations for each profile, trying to create viable solutions. Therefore, all configurations were made aiming to have 15 kg of mass.

It will be verified if the structure can be submitted to the efforts by checking if Von Mises tension is below yield strength.

Table 3.4 shows the structure designed with each profile, and the mesh parameters utilized as well as the time to complete meshing. In table 3.5, it can be seen how the forces will deform the structure despite being exaggerated. Lastly in table 3.6, the maximum Von Mises tension is exposed as well as the parts of each structure that are not under a safety factor, accordingly with Von Mises tension criterion, of 5.

Table 3.4. Different structures and meshing details.

Profile size: [mm]	Stucture assembly:	Mass: [kg]	Element Size [mm] / Tolerance [mm]	Total Nodes / Total Elements	Time to complete meshing: [hh:mm:ss]
 20	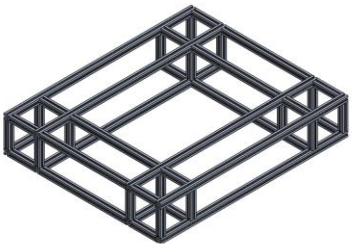	6.45	2.72	7976495	37:18
			0.14	4770623	
 30	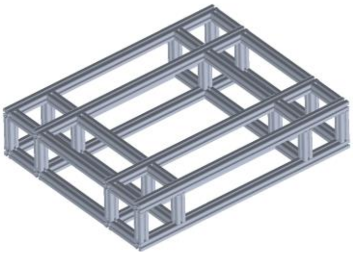	14.41	3.61	5578979	14:11
			0.18	3309538	
 40 light	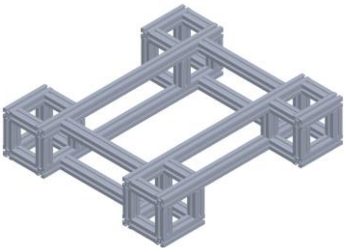	15.89	4.35	4327938	17:59
			0.22	2481212	
 40	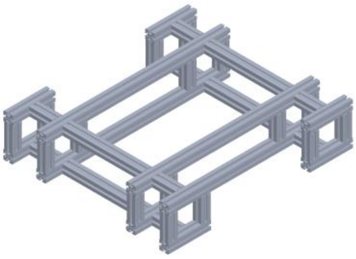	20.87	4.53	3507624	7:21
			0.23	2093278	

Table 3.5. Displacement results.

Profile size: [mm]	**Displacement Result Top view::**	**Def max: [mm]**	**Relation Mass*Deformation**	**Solution time: [hh:mm:ss]**
 20	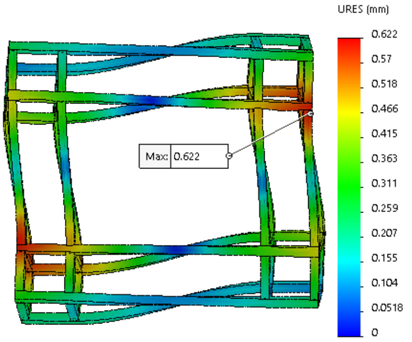	0.62	4.01	20:09
 30	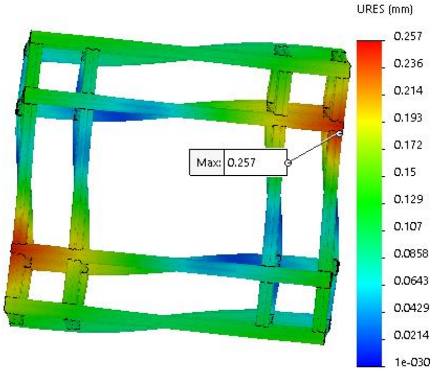	0.26	3.70	13:07
 40 light	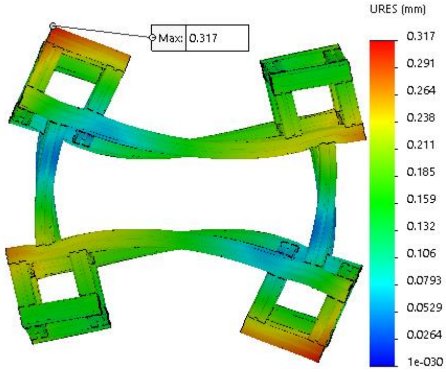	0.32	5.04	7:11
 40	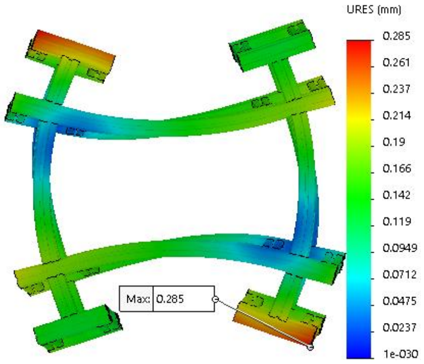	0.29	5.95	6:14

Table 3.6. Factor of safety, Maximum Von Mises tension criterion.

Profile size: [mm]	Stucture assembly:	Detail:	Max. Von Mises Tension: [MPa]
 20	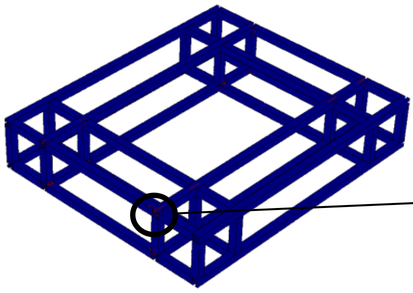	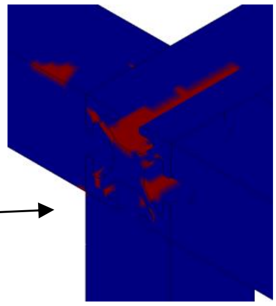	171
 30	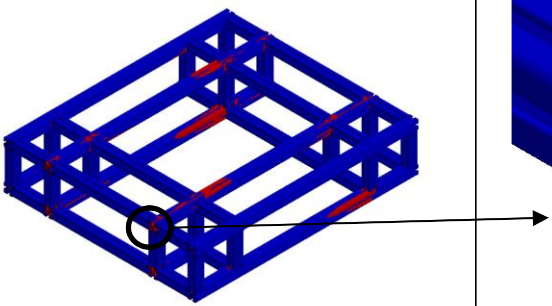	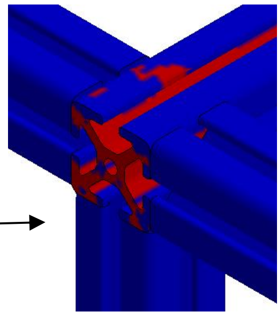	60.3
 40 light	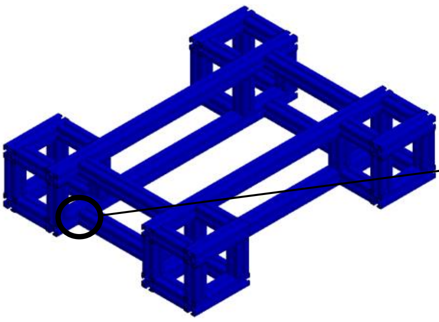	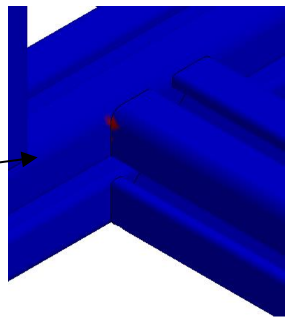	136
 40	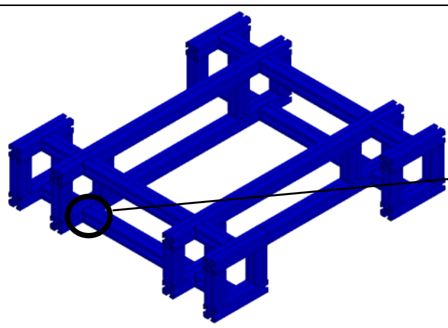	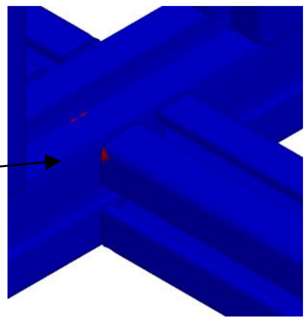	80

* In red, the areas where the factor of safety of 5 doesn't apply. In blue the material is above the factor of safety.

** Detail was chosen where it was more red areas

The 20 mm profile utilized in this study is different than the real one, which has a form like the 30 or 40 mm profile. Despite that simplification used, the meshing time is still much longer than the others. Results with this profile might be optimistic because the profile should have a hole in the middle and edges in corners, which means less material.

The size of the element utilized increased with the size of the profiles. Comparing both profiles with 40 mm, the light profile has less element size because it is more complex.

Looking at the mass of the structures, the structure created with the 40 mm profile has approximately 40% more mass than the criterion of having approximately 15 kg.

The way that structures deformed is as expected after doing similar simulations in annex A. However, the relation between mass and deformation is different from the corresponding structure in the same annex. That difference should be due to the change of profile size and the shape of the profile.

The 20 mm structure has nearly double maximum deformation than the others structures. In table 3.5, the maximum deformation is only close to the maximum tension (195 MPa) for the 20 mm structure which confirms that this structure is not good enough for this project.

A safety factor study was also performed according to Von Mises criterion. The 20 mm and 30 mm profiles had lots of areas without respecting a safety factor of five. On the other hand, 40 mm light and 40 mm profile had residual places which were not respecting this safety factor.

To summarise, the structure with 40 mm light profile had not only a good result for maximum deformation and respected a safety factor of five for maximum tension but also a very reasonable mass. Further on, it will be shown that bigger profiles use bigger screws which means stronger connections.

3.3.4. Connections

Item catalogue fastening technology [38] suggest the usage of those three standard types of connections (figure 3.12) for displacement forces, torsional moment and bending moment.

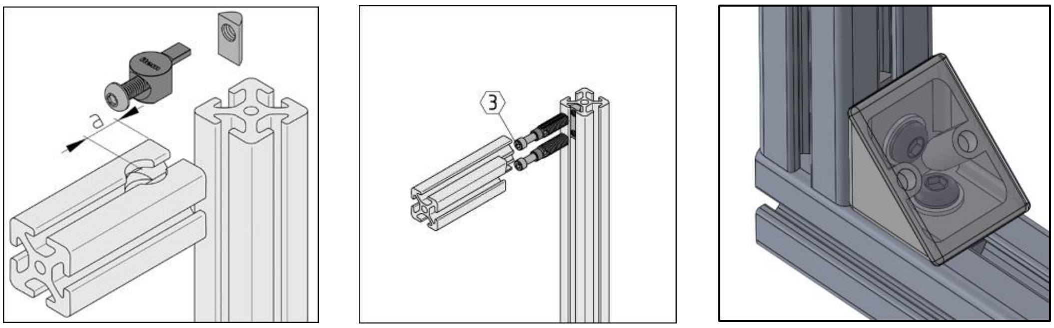

Figure 3.12. Automatic-Fastening, Universal-Fastening, Angle Bracket **[38]**.

First two fastenings shown above require machining, for that reason, it is not so easy to change the disposition of the structure. The angle bracket fastening doesn’t need any cuts and it adds very rigid material to a right-angle connection providing rigidity and fixation.

To quantifying the improvement in the structure´s stiffness, it was made a simulation with and without this fastening (figure 3.13). The simulation follow the exact same characteristics as the previous ones, but it was done in only one quarter of the structure, and with draft quality mesh because this parts increase the complexity of the mesh. Therefore, the use of draft quality mesh was the only way to make this study to work, but SolidWorks advice to be careful with results provided by this kind of mesh, because it has less precision. We will just compare the results to have an idea of the difference provided by these fastenings.

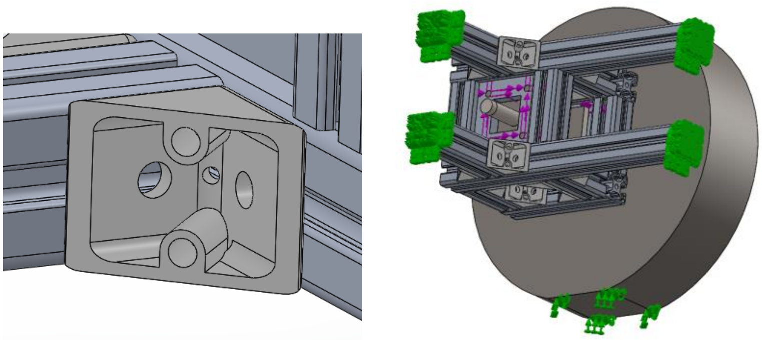

Figure 3.13. Automatic-Fastening, one quarter of the structure with restrictions in green and forces in purple.

Deformation results are expressed bellow in figure 3.14, were we can see a similar deformation distribution around the structure, but with different maximum values. Without the fastenings we have 0.164 mm deformation and with them we have 0.123, which means a decrease of 25% of maximum deformation.

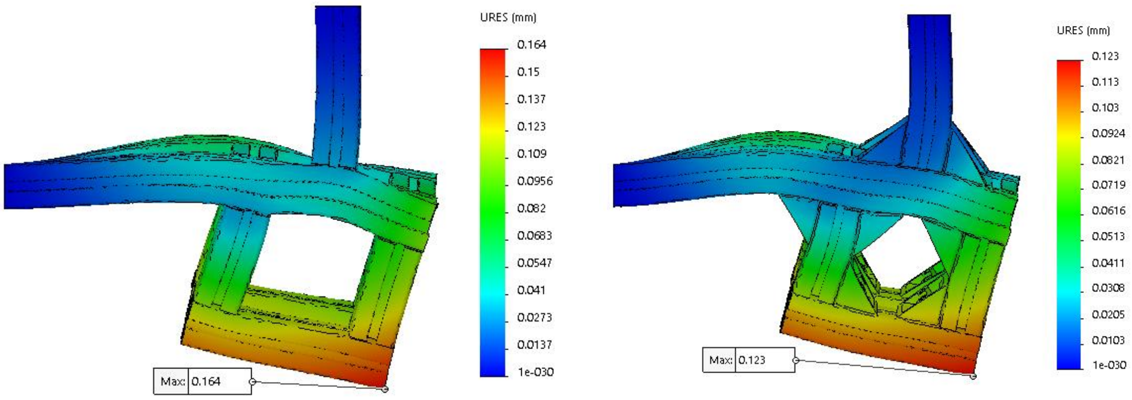

(a) (b)

Figure 3.14. Deformation results, top view: a) Without fastenings and b) with fastenings.

One of the main topics for choosing the right profile size is how strong the connections are, that is mainly due to the screws used. In the table 3.7 it is shown how much force can safely be applied in different profile sizes. Note that 5 correspond to 20 mm profile, 6 to 30 mm profile and 8 to 40 mm profile. It was calculated the biggest restriction has having 2666 N. Even if this force was only carried by one screw, using line 8, light version of the profile, it would be safe.

Table 3.7. The permissible tensile forces F on the groove flanks. These nominal loads include safety factors (s > 2) against plastic deformation **[39]**.

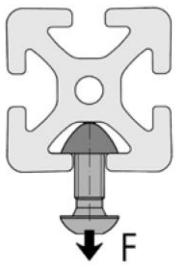

Groove shape	5	6	8
Normal	500N	1750N	5000N
Light		500N	2500N
E			1750N

3.4. Final assembly and manufacturing technologies

Most of the products used will be standard products, selected from catalogues, like belts, pulleys, couplings and general structure parts. However, connections between bearings and the structure or support sheets for controllers, batteries, motors and other electronic parts will be made for this exact purpose, designed for this project (figure 3.15).

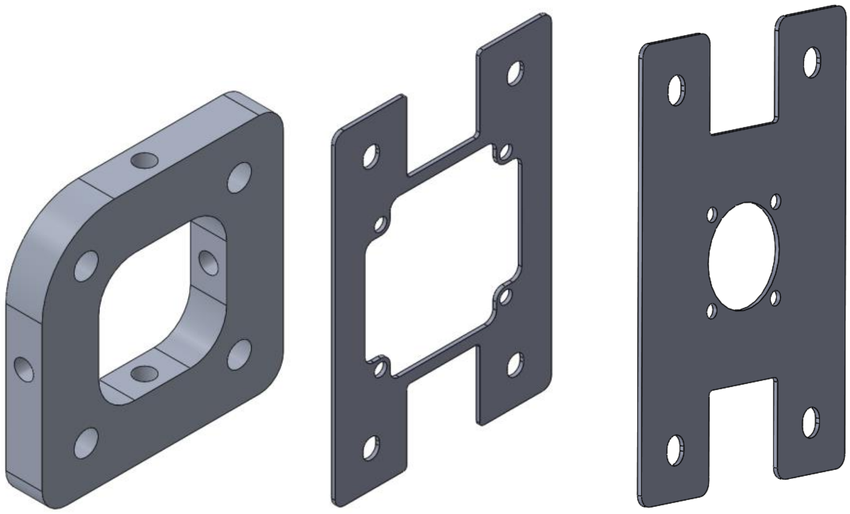

Figure 3.15. Components designed and manufactured, 2D designs in appendices.

Pieces that connect the bearings to the structure, which are very important for alignment of the shafts are going to be made using CNC milling. All sheets made for connecting parts to the structure will be made using cut by water jet or laser.

Although this is mostly an outdoor robot, it was always a goal that there was mobility also inside a building. To do so, due to the selection of very compact pulleys and couplings and the shortening of the structure, the robot is only 830 mm wide.

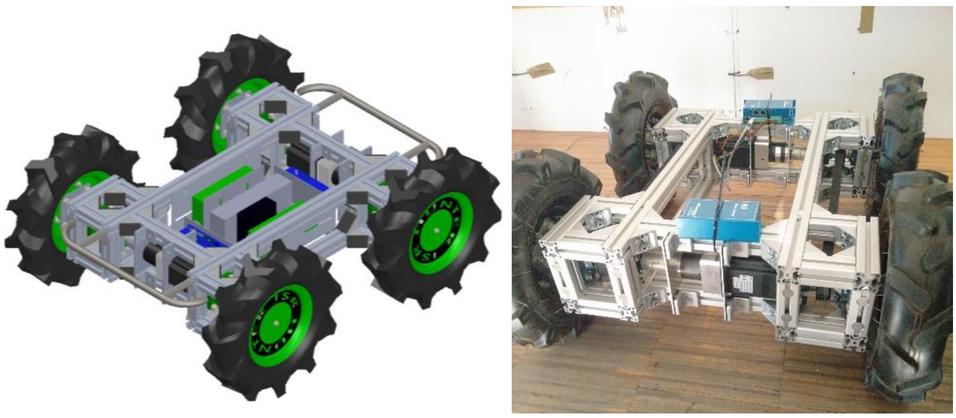

Figure 3.16. Final assembly.

4. TESTS AND RESULTS

4.1. Test of movement in different solos and resolution of problems

The prototype was tested firstly indoors, where it could make all movements including rotating around itself (figure 4.1). It could also get through the elevator door which was one of the main restrictions and could pass in some doors that make really easy to take it outside.

Figure 4.1. Video frames of the robot rotating around itself.

The robot was also tested on other types of soil, such as concrete, tar and terrain (figure 4.2), having been able to perform normal movements and even climbing ramps with relative ease.

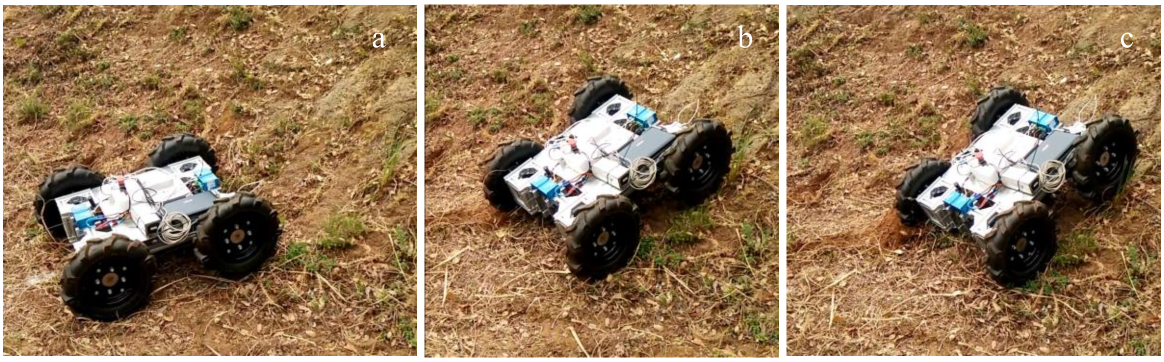

Figure 4.2. Video frames of the robot climbing in terrain.

Unfortunately, after a few minutes testing the robot on sloping ground, one of the shafts broke (figure 4.3). In this case the problem was in the insufficient welding made that was the fragile point that originated this problem.

Then the robot was able to continue to move by itself back to the laboratory with only three wheels, still being able to make all the necessary movements and even to rotate around itself. The robot was dismounted and a repair was done in all shafts (figure 4.3).

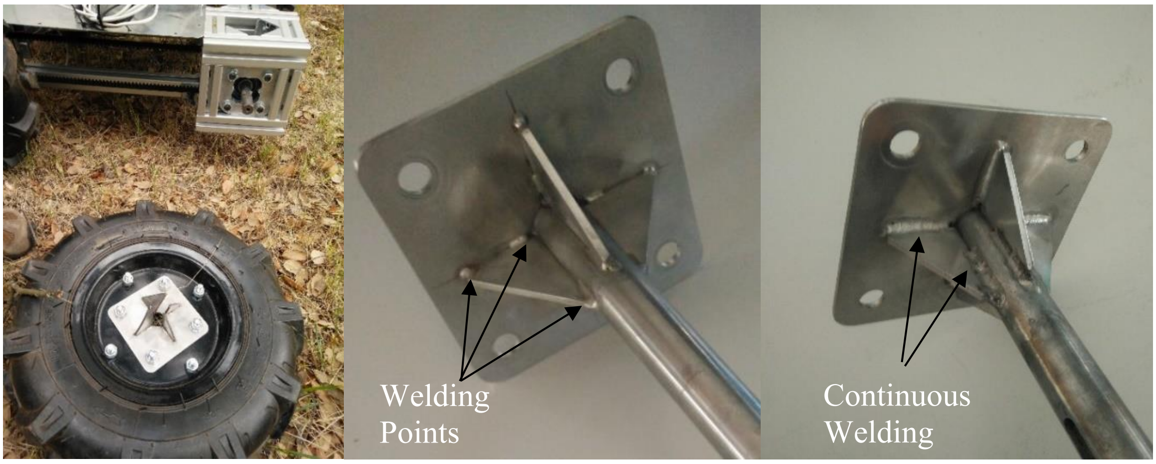

(a) **(b)** **(c)**

Figure 4.3. First problem, testing in rough conditions: a) Broken wheel, b) Shaft before new welding, c) shaft after new welding.

4.1. Testing robot limits and obtaining final specifications

After fixing some misalignments due to the first inexperience assembling, the robot was ready for new experiments. Despite the project initial specifications did not included that the robot should be ready to climb stairs, it was made with a ground clearance big enough to it make possible.

The biggest steps it was able to climb are shown in figure 4.4. It was also tested in standard steps (180x270 mm) but it could not climb.

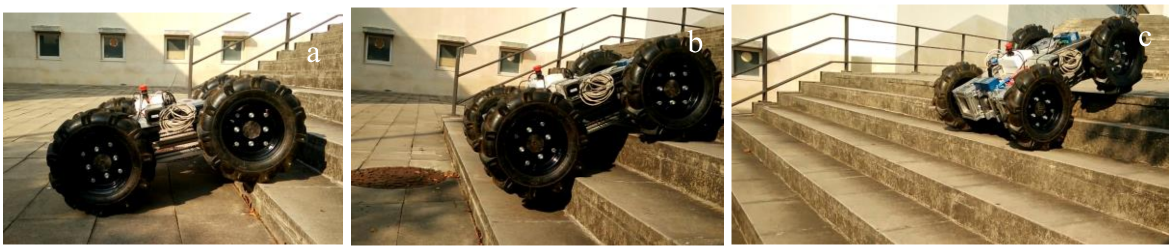

Figure 4.4. Hunter climbing steps with 170x370 mm.

The maximum velocity was measured as 0.88 m/s but theoretical it should be able to achieve 1.6 m/s.

After some tests in ramps, steps and in different solos, the robot did climb a 200 mm step (figure 4.4), which should be around the maximum it can do. The robot could also climb a ramp with average inclination of 30º (figure 4.5), which was the highest inclination found in the testing field.

(a) **(b)**

Figure 4.5. Challenging Hunter: a) climbing 30º slope, b) climbing a 200 mm step.

Tests have revealed that the robot is not prepared for significant impacts, especially if it occurs on only one wheel. It was also possible to identify the fixation of the shafts as a weak point of the robot since the bearings were reused of the previous robot and apparently are not suitable.

The payload will be measured as soon as the robot has a cover and a shelf for electronic parts that are now on top of the robot, which is already projected and will make easier to put well distributed loads on top of it.

To summarise, table 4.1 has the characteristics of the robot developed in this dissertation.

Table 4.1. Hunter characteristics.

	Weight (kg)	Payload (kg)	Max. Speed (m/s)	Width (mm)	Ground Clearance (mm)	Climb Stairs	Modular	Omni-directional
Hunter	75*	100*	0.88	830	110	Yes**	Yes	No

* Theoretical values, not yet tested
** 170 mm high or less and 370 mm wide or more

5. CONCLUSIONS

In this dissertation, it was proposed the development of a structure for a mobile outdoor robot. This structure was designed, simulated, perfected, fabricated and tested. Although it focused on the structure, in order to design and test the robot, it was necessary to design and acquire all the necessary components for the project including pulleys, belts, couplings, among others.

The structure was made with aluminium profiles achieving the creation of a modular and reconfigurable structure. Their complexity was an extra challenge for the simulation using finite element analysis. Before making the necessary simulations to verify the stiffness of the structure, the forces to which the structure was subjected were studied, having been understood that the rotation around itself is the critical moment.

It was concluded that using a standard mesh would be the better option to simulate the developed model and that the deformation would be the result to be taken into account since the created tensions will be far from the yield strength. After simulating several structures with various profile sizes, was selected the one that guaranteed a mass within the objective, a maximum reasonable deformation and still has a safety factor according to the criterion of Von Mises of five.

During the tests, it was possible in the first phase, to detect and correct some weak points and in a second phase, to confirm the ability of the robot to move on all types of terrain. In addition, due to its compact design, it can pass through all the doors needed to enter and exit the building. An attempt was made to climb stairs, but it was only possible to complete the ascent with steps of 170 mm height and 370 mm width. The vehicle has reached a maximum speed of 0.88 m / s, but it is expected to be able to reach 1.64 m/s with some changes in controller’s settings and use of more powerful batteries. The robot was still able to climb a slope of 30º, proving its high traction.

The changes in transmission mechanisms relative to the previous robot resulted in less deformations and smoother movement.

5.1. Future work

In the appendices, there is a design named ‘covers and compartment for electronic components’ that contains a compartment to properly assemble all electronic components and a top and a bottom cover for the robot. The idea is to be able to mount and dismount these parts in the main structure. It would be an improvement if these parts were manufactured and successfully tested.

As the developed robot is modular and reconfigurable, it would be a good challenge to not only be able to change its structure, but also be able to change his locomotion mechanism. In this scope, it is suggested the possibility to adapt the platform to move with a tracked mechanism.

BIBLIOGRAPHY

[1] "Tiramisu - Humanitary demining toolboc," [Online]. Available: http://www.fp7-tiramisu.eu/. [Accessed 17 5 2017].

[2] G. Cabrita, R. Madhavan and L. Marques, "A Framework for Remote Field Robotics Competitions," *Autonomous Robot Systems and Competitions (ICARSC), 2015 IEEE International Conference on. IEEE, 2015..*

[3] R. Siegwart and I. R. Nourbakhsh, "Introduction to Autonomous Mobile Robots", The MIT Press, Massachusetts Institute of Technology, Cambridge, Massachusetts, 2004.

[4] Ingeniarius, [Online]. Available: http://ingeniarius.pt/?page=forte#. [Accessed 11 07 2017].

[5] Mars rover, [Online]. Available: https://en.wikipedia.org/wiki/Sojourner_(rover). [Accessed 11 07 2017].

[6] Boston Dynamics, [Online]. Available: https://www.bostondynamics.com/sandflea. [Accessed 11 07 2017].

[7] NASA , [Online]. Available: http://www.frc.ri.cmu.edu/projects/pioneer/. [Accessed 11 07 2017].

[8] Bosch, [Online]. Available: https://www.deepfield-robotics.com/en/BoniRob.html. [Accessed 11 07 2017].

[9] Saga Robotics, [Online]. Available: https://sagarobotics.com/blogs/news/162130055-w-series-br-working-horse-pure-power. [Accessed 11 07 2017].

[10] L. Marques, A. T. d. Almeida, M. Armada, R. Fernández, H. Montes, P. González and Y.Baudoin, "State of the Art Review on Mobile Robots and Manipulators for Humanitarian Demining," in IARP WS on Humanitarian Demining, Sibenik, Croatia (2012).

[11] Nomad 4WD Off-Road Chassis kit, [Online]. Available: https://www.servocity.com/nomad. [Accessed 24 07 2017].

[12] Gear eds, [Online]. Available: https://www.amazon.com/Robot-Platforms/b/ref=dp_bc_4?ie=UTF8&node=8498890011. [Accessed 24 07 2017].

[13] Hangfa Hydraulic Engineering, [Online]. Available: http://www.robotshop.com/ca/en/hangfa-navigator-c2-robot-platform.html. [Accessed 24 07 2017].

[14] Inspectorbots, [Online]. Available: http://www.inspectorbots.com/Mega_Bot.html. [Accessed 24 07 2017].

[15] Clearpath, [Online]. Available: https://www.clearpathrobotics.com/warthog-unmanned-ground-vehicle-robot/. [Accessed 11 07 2017].

[16] O. J. Bawden, Design of a lightweight, modular robotic vehicle for the sustainable intensification of broadacre agriculture, Diss. Queensland University of Technology,

2015..

[17] Austrian Institute of Technology, [Online]. Available: http://s630617833.online.de/works/modular-mobile-robot-ait. [Accessed 11 07 2017].

[18] L. Got, "Design and Development of Modular Multipurpose Omnidirectional Autonomous Mobile Robotic Platform for Remote Farming Application," Master´s Thesis in Mechatronics, 2015.

[19] makeblock, [Online]. Available: http://store.makeblock.com/. [Accessed 11 07 2017].

[20] K. Goris, "Autonomous mobile robot mechanical design.," VrijeUniversiteitBrussel, Engineering Degree Thesis, Brussels, Belgium (2005)..

[21] Adept, [Online]. Available: http://www.mobilerobots.com/ResearchRobots/Seekur.aspx. [Accessed 24 07 2017].

[22] Dr. Robot, [Online]. Available: http://www.robotshop.com/en/dr-robot-jaguar-4x4-mobile-platform-chassis-motors.html. [Accessed 24 07 2017].

[23] Dagu, [Online]. Available: https://www.amazon.com/gp/product/B00C0Q672M/ref=as_li_tl?ie=UTF8&camp=1789&creative=390957&creativeASIN=B00C0Q672M&linkCode=as2&tag=intorobo-20&linkId=7MY63FJZR4NQ3MSM. [Accessed 24 07 2017].

[24] Super droid robots, [Online]. Available: https://www.amazon.com/SuperDroid-Robots-Terrain-Robot-Platform/dp/B00CFQWE5Q/ref=sr_1_3?s=industrial&ie=UTF8&qid=1496315595&sr=1-3&keywords=6WD. [Accessed 24 07 2017].

[25] Super Droid Robots, [Online]. Available: https://www.superdroidrobots.com/shop/item.aspx/new-custom-rc-6wd-robot-with-snow-plow/1612/. [Accessed 24 07 2017].

[26] Lee, K. C. H., S. H., Kang, S. C., Kim, M. S., Kwak and Y. K, "Double-track mobile robot for hazardous environment applications," *Advanced Robotics,* pp. 447-459, 2003.

[27] King Kong Robot, [Online]. Available: http://www.robotshop.com/en/super-size-hd-tracked-tank-robot-kit.html. [Accessed 27 07 2017].

[28] Dr. Robot, [Online]. Available: http://www.robotshop.com/en/jaguar-v4-tracked-mobile-robotic-platform.html. [Accessed 27 07 2017].

[29] Robotshop, [Online]. Available: http://www.robotshop.com/en/xbot-all-terrain-tracked-mobile-robot.html. [Accessed 11 07 2017].

[30] A. Afanador, "Triangle track vehicle wheel". U.S. Patent No. 8,695,735. 15 Apr. 2014.

[31] S. D. Potter, "Omni-directional wheel". Patent US 7980335 B2, 26 Jan 2009.

[32] Vehicle Technologies Inc., [Online]. Available: http://www.vetexinc.com/applications/mobilerobots.html. [Accessed 11 07 2017].

[33] A. Buchstab, "Mobile Robot". Patent US 20130226340 A1, 22 Fev 2013.

[34] KUKA, [Online]. Available: http://www.youbot-store.com/. [Accessed 27 07 2017].

[35] KUKA, [Online]. Available: https://www.kuka.com/en-de/products/mobility/mobile-robots/kmr-iiwa. [Accessed 27 07 2017].

[36] RobotShop, [Online]. Available: http://www.robotshop.com/en/hangfa-navigator-q2-robot-platform.html. [Accessed 11 07 2017].

[37] S. Dogru and L. Marques, "Power Characterization of a Skid-Steered Mobile Field Robot," *Autonomous Robot Systems and Competitions (ICARSC), 2016 International Conference on. IEEE, 2016.*.

[38] Item, "Overview – finding the right fastener fast," [Online]. Available: http://catalog.item24.com/images/medienelemente/DOK/DATA/DOK_DATA_weg-zur-richtigen-Verbindung__SEN__AIN__V3.pdf. [Accessed 11 9 17].

[39] Item, "Technical data for profiles," [Online]. Available: http://catalog.item24.com/images/medienelemente/DOK/DATA/DOK_DATA_profil-tech-daten__SEN__AIN__V3.pdf. [Accessed 11 9 17].

ANNEX A

In this part, some viable structures will be simulated to support the concept shown in figure 3.4, all of which are developed with 40 mm profiles. The only change is the configuration of the structure that will result in different behaviors responding to the solicitations, which were previously described.

Table A.1. Comparison of different types of structures.

Profile 	Displacement Result Top view:	Mass: [kg]	Def max: [mm]	Relation: Mass * Deformation
1 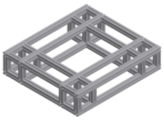	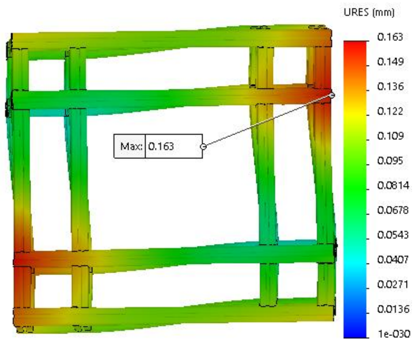	30.49	0.16	4.97
2 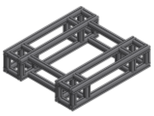	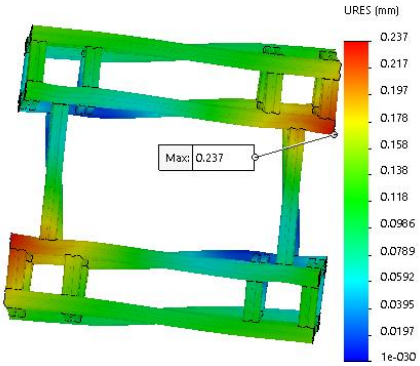	27.86	0.24	6.60
3 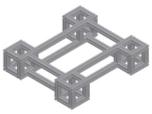	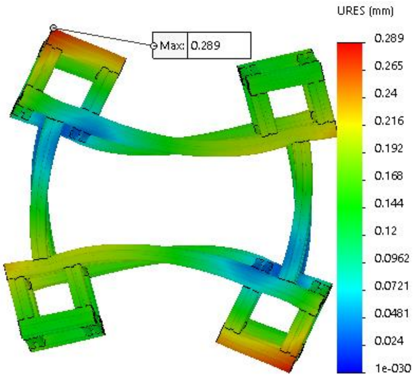	22.87	0.29	6.61
4 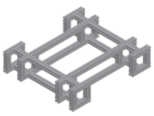	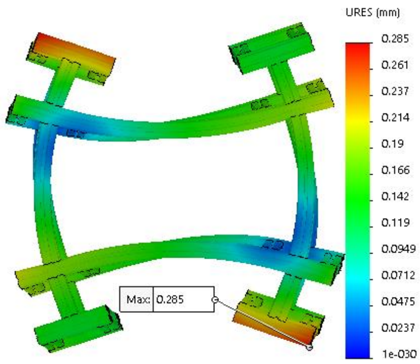	20.86	0.29	5.95

Firstly, we can observe that the first two structures have a more homogeneous deformation whereas the structure three and four has quite flexion in the longer bars.

The maximum deformation is smaller in the heavier structure and that it increases with the decrease of the mass of the structures, except for the last structure that presents practically the same deformation as the penultimate one.

Structure one is the one with the best mass deformation relation and a more homogeneous deformation, while the second structure shows a small decrease in mass compared to the increase in maximum deformation relative to structure one. Structures two and three have smaller mass than the first, and structure four despite having the same deformation as structure three and less mass, has the problem of only having two bars connecting each bearing at the ends to the main frame, which causes the connections to become fragile.

APPENDICES

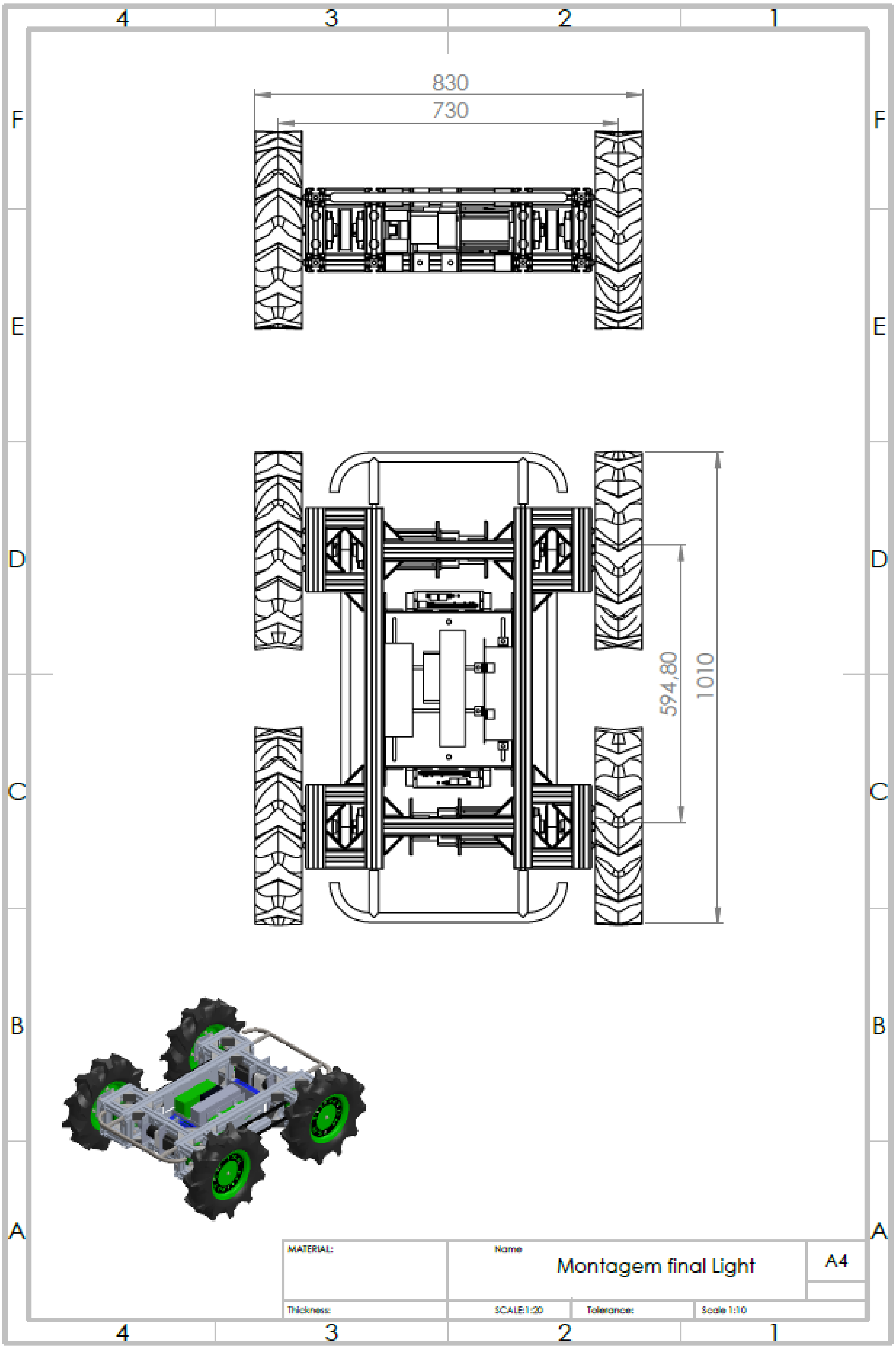

830
730
594,80
1010
MATERIAL:
Name
Montagem final Light
A4
Thickness:
SCALE:1:20
Tolerance:
Scale 1:10

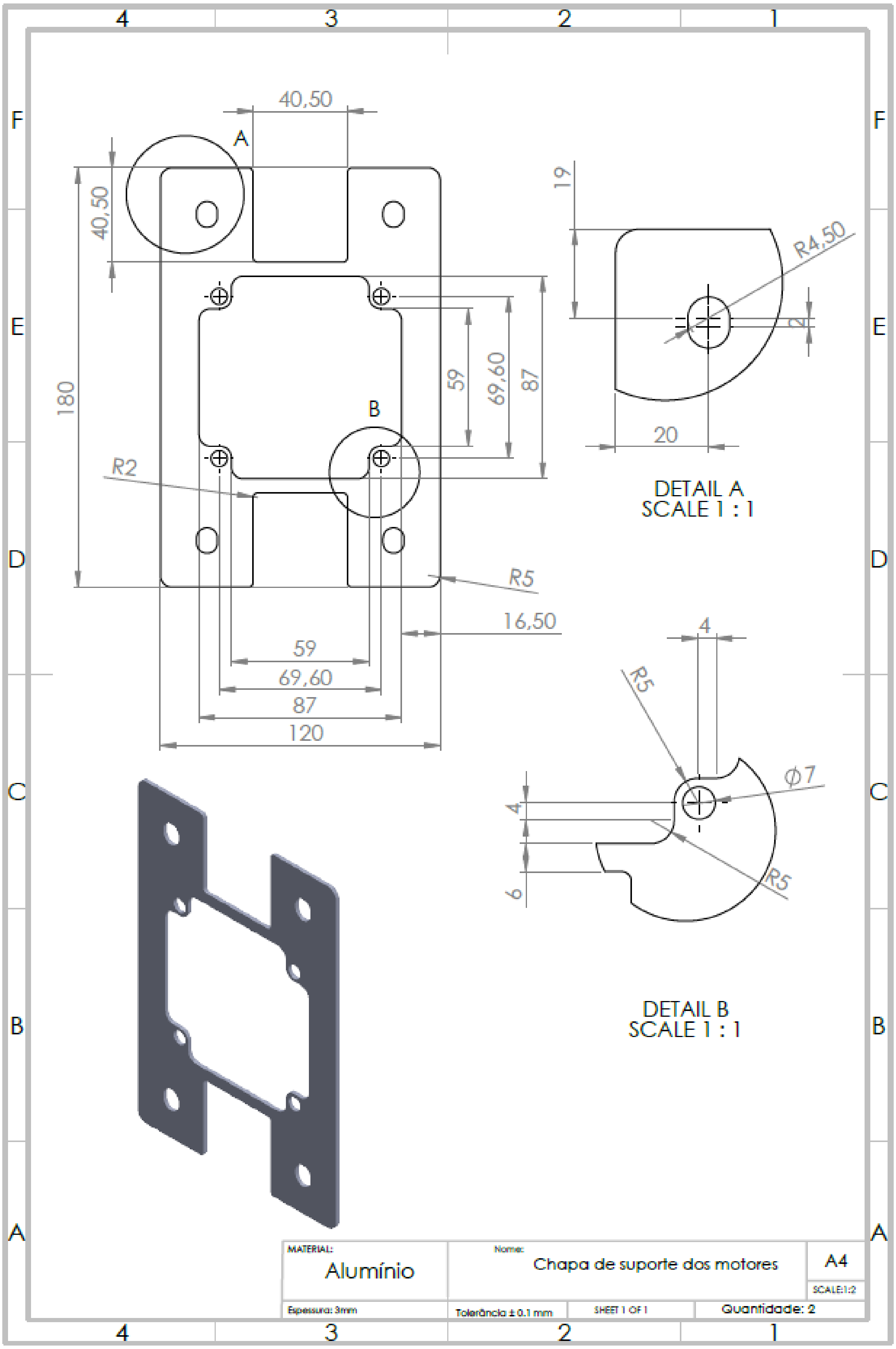
40,50
A
40,50
180
R2
B
59
69,60
87
19
R4,50
2
20
DETAIL A
SCALE 1 : 1
R5
16,50
59
69,60
87
120
4
R5
Ø7
4
6
R5
DETAIL B
SCALE 1 : 1
MATERIAL:
Alumínio
Nome:
Chapa de suporte dos motores
A4
SCALE:1:2
Espessura: 3mm
Tolerância ± 0.1 mm
SHEET 1 OF 1
Quantidade: 2

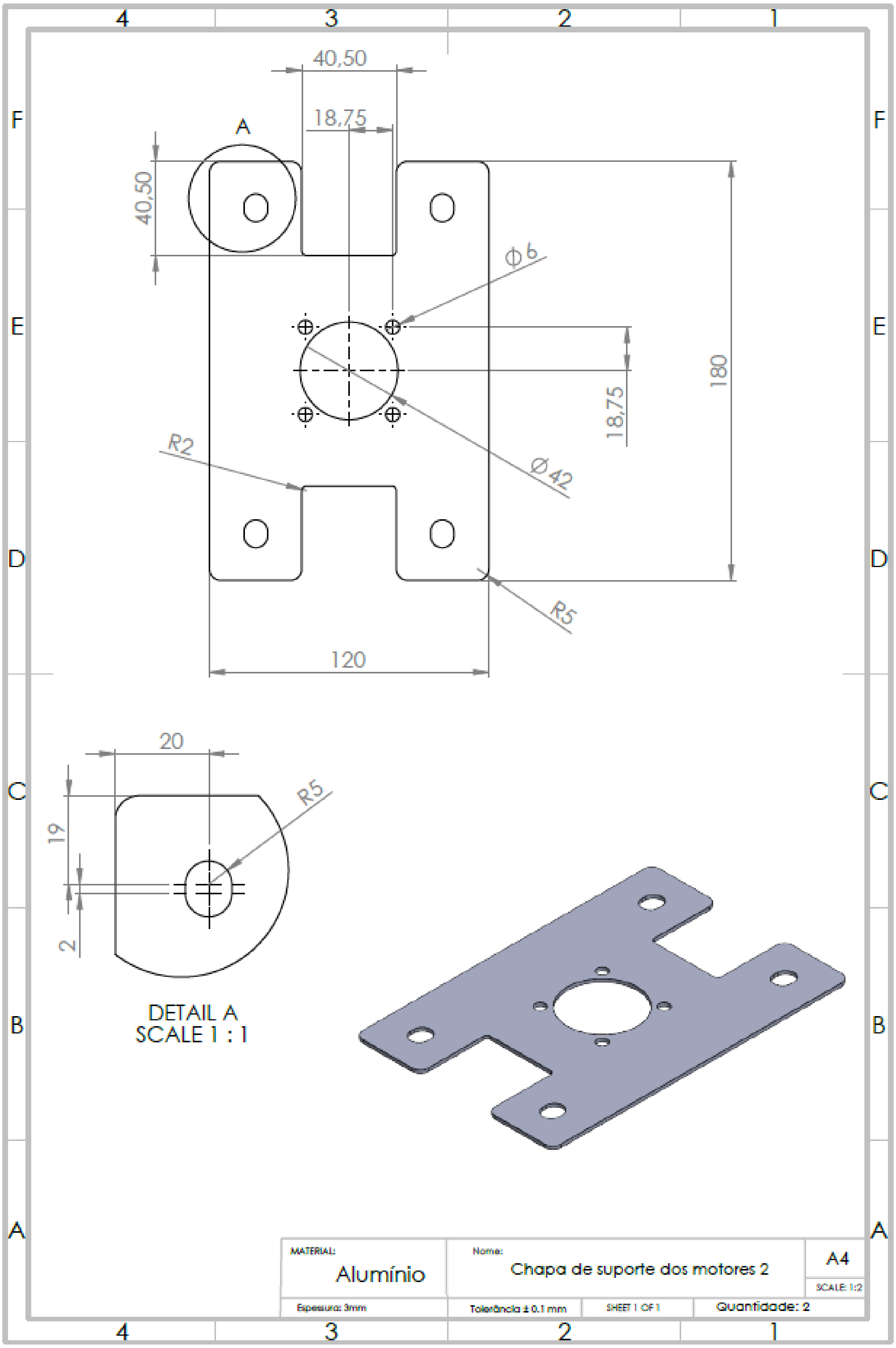
4
3
2
1
F
E
D
C
B
A
40,50
18,75
A
40,50
Φ6
18,75
180
R2
Ø42
R5
120
20
R5
19
2
DETAIL A
SCALE 1 : 1
MATERIAL:
Alumínio
Nome:
Chapa de suporte dos motores 2
A4
SCALE: 1:2
Espessura: 3mm
Tolerância ± 0.1 mm
SHEET 1 OF 1
Quantidade: 2

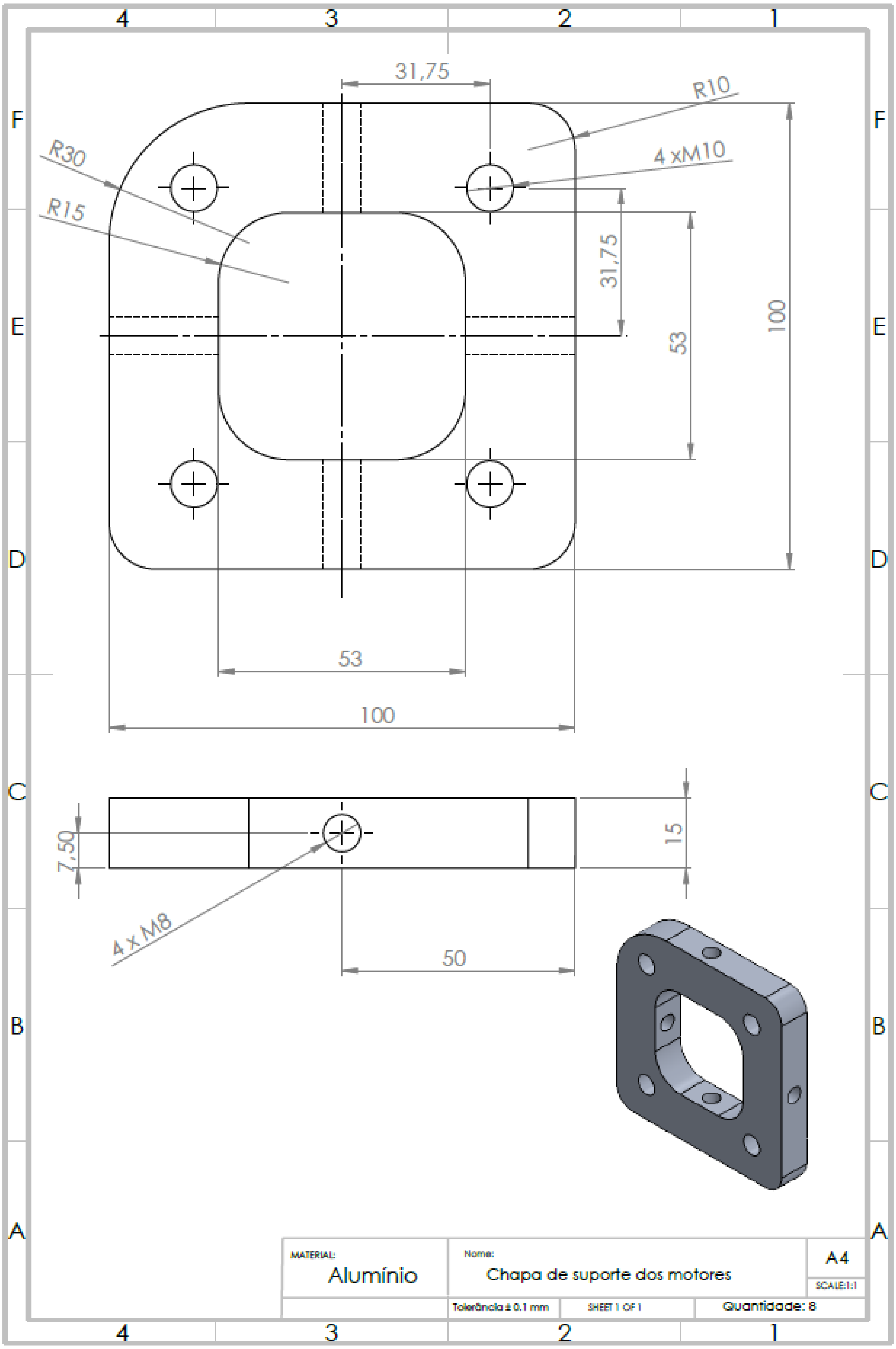

31,75
R10
R30
4 xM10
R15
31,75
53
100
53
100
7,50
15
4 x M8
50
MATERIAL:
Alumínio
Nome:
Chapa de suporte dos motores
A4
SCALE:1:1
Tolerância ± 0.1 mm
SHEET 1 OF 1
Quantidade: 8

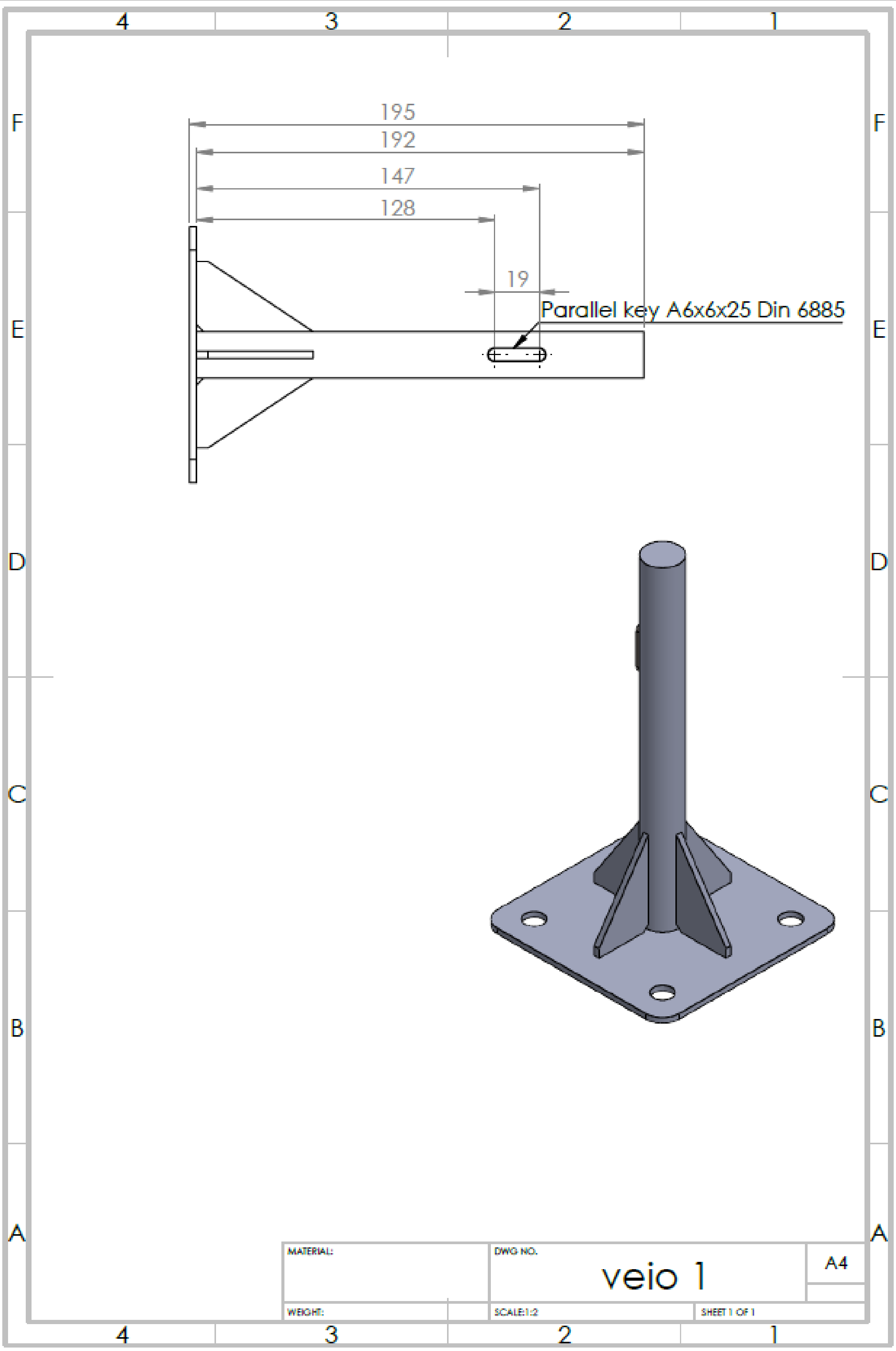
4
3
2
1
F
E
D
C
B
A
195
192
147
128
19
Parallel key A6x6x25 Din 6885
MATERIAL:
DWG NO.
veio 1
A4
WEIGHT:
SCALE:1:2
SHEET 1 OF 1

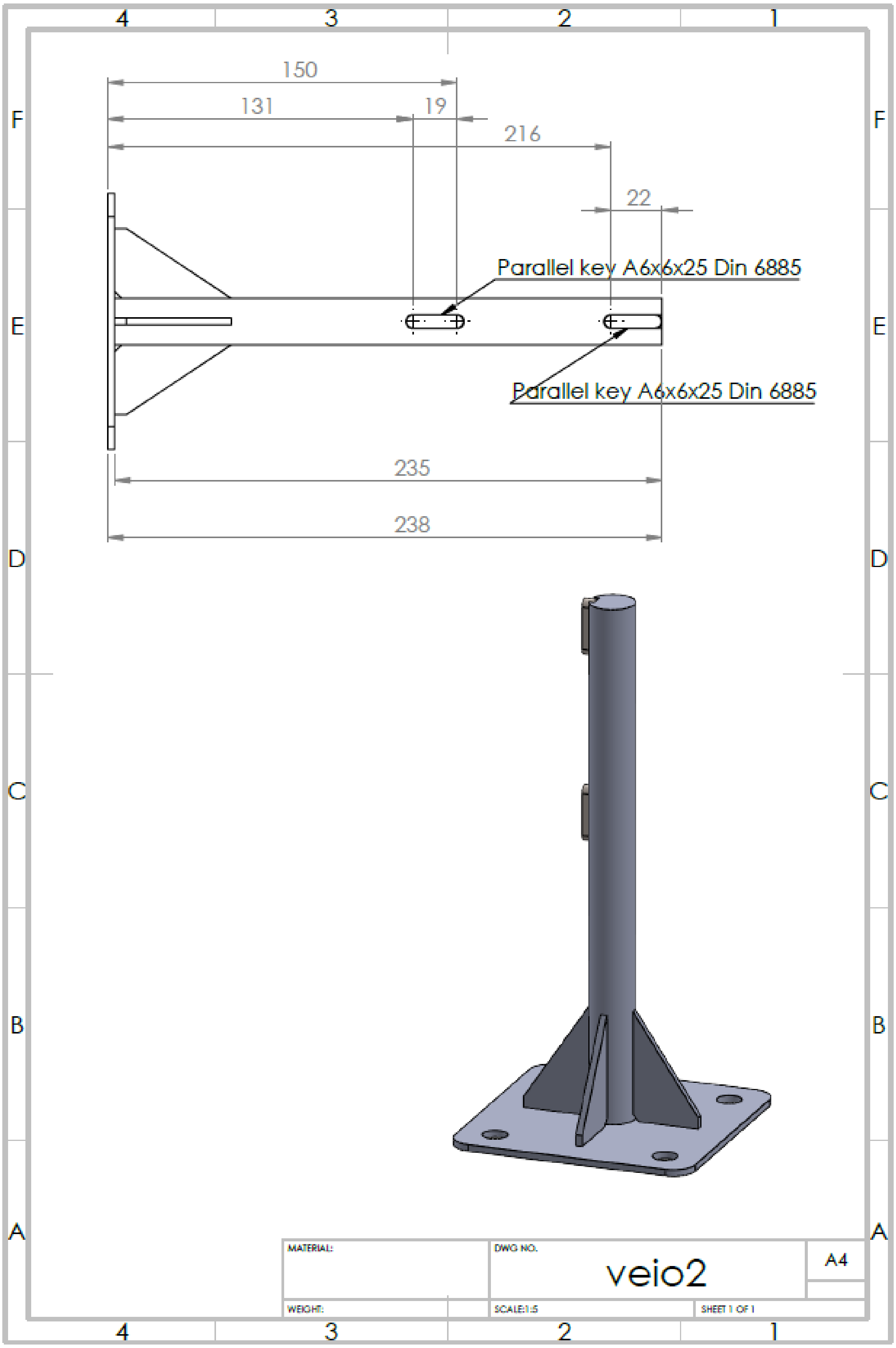
4
3
2
1
F
E
D
C
B
A
150
131
19
216
22
Parallel key A6x6x25 Din 6885
Parallel key A6x6x25 Din 6885
235
238
MATERIAL:
DWG NO.
veio2
A4
WEIGHT:
SCALE:1:5
SHEET 1 OF 1

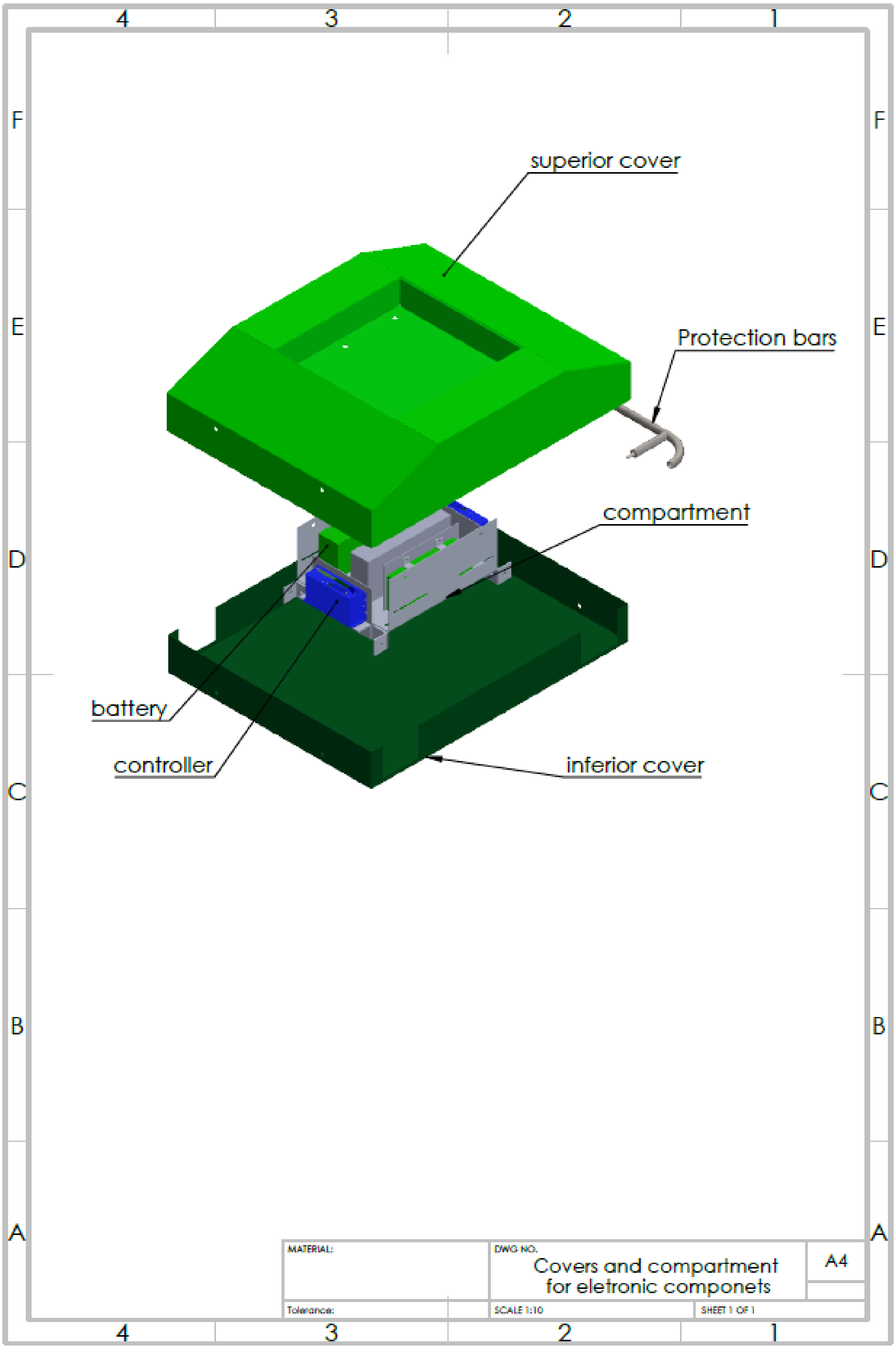
4
3
2
1
F
E
D
C
B
A
superior cover
Protection bars
compartment
battery
controller
inferior cover
MATERIAL:
DWG NO.
Covers and compartment
for eletronic componets
A4
Tolerance:
SCALE 1:10
SHEET 1 OF 1